

1 **Interactive comment on "Daytime formation of nitrous acid at a coastal remote site in Cyprus**
2 **indicating a common ground source of atmospheric HONO and NO" by Meusel et al.**

3

4 **Anonymous Referee #1**

5

6 **General comments:**

7 *In this manuscript the authors present results of HONO and other trace gas species from a study performed in*
8 *Cyprus as part of the CYPHEX campaign in 2014. During the measurement period they observed a high HONO/NO_x*
9 *ratio and a large daytime source of HONO. A budget analysis is performed and a missing source of HONO up to 3.4*
10 *$\times 10^6$ molecules $\text{cm}^{-3} \text{s}^{-1}$ calculated, which is comparable to values reported in mountain and forest sites. Under*
11 *humid conditions the HONO source correlates well with NO and the authors attribute this missing HONO source to*
12 *emissions from soil. Finally, the impact of the HONO on OH production rates is calculated and the results show that*
13 *the HONO photolysis contributes, on average, 30% to OH production during the morning and evening.*
14 *Understanding the daytime source of HONO is important due to its role in OH formation and this study provides*
15 *important data on HONO sources in a location which is not strongly impacted by combustion sources.*
16 *The manuscript is well written, with appropriate sections and easy to follow. I recommend the manuscript for*
17 *publication in ACP after addressing the comments below:*

18 **Response:**

19 We thank the reviewer for the positive evaluation and please find our point-to-point responses as listed below.

20

21

22 **Specific comment:**

23 *One of the main concerns is that no uncertainty analysis has been performed for the HONO/NO_x ratios or the*
24 *HONO budget and calculation of the missing HONO sources. This should include instrument uncertainties in the*
25 *HONO and NO_x measurements along with errors in the PSS calculation. It would then be beneficial to include error*
26 *bars on Figure 5a and b, to show the upper and lower limits to the estimated unknown HONO source.*

27 **Response:**

28 Following the reviewer's suggestion, we now state all instruments' uncertainties in the revised manuscript. The
29 uncertainty of LOPAP (HONO) is 10%, based on the uncertainties of gas and liquid flow rates, regression of the
30 calibration curve, and calibration standard solutions (manual of LOPAP, QUMA 2004). The accuracy (2 sigma)
31 of the OH measurements was 29% and the precision (1 sigma) was 4.8×10^5 molecules cm^{-3} (personal contact with
32 Harder et al., hartwig.harder@mpic.de). The instrument uncertainties for NO, NO₂, O₃, J were already stated in
33 the original manuscript (20%, 30%, 5%, 10%, personal contact with Fischer et al, horst.fischer@mpic.de and
34 Crowley et al., john.crowley@mpic.de).

35 According to Gaussian error propagation, these instrument uncertainties affect the calculation of the unknown
36 HONO source S_{HONO} with about 16%.

37 We agree that error bars would help to indicate the uncertainty of the source and sink terms in our calculations.
38 As Fig. 5 a and b show half-hourly mean values of diurnal patterns, we prefer to show the standard deviation of
39 the diurnal mean values as error bars, now included in Fig. 5 a and b, and to discuss the uncertainties in the text.

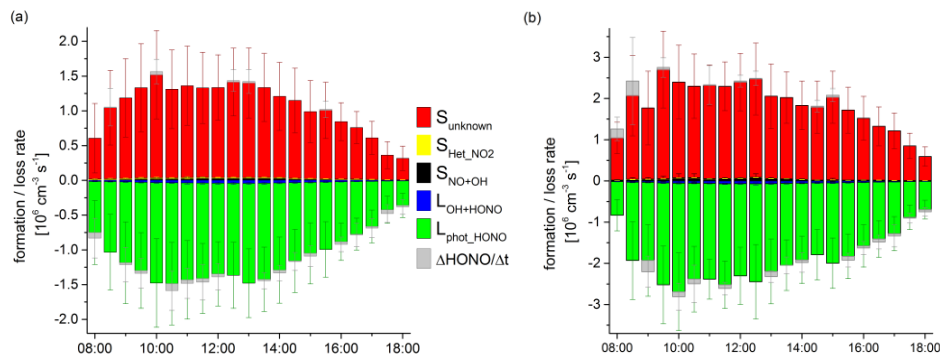
40 We now added in the revised versions of the manuscript:

41 page 4 line 13-15: "The accuracy of the HONO measurements was 10%, based on the uncertainties of liquid and
42 gas flow, concentration of calibration standard and regression of calibration ."

43 page 4 line 36-37: "The accuracy (2 sigma) of the OH measurements was 29% and the precision (1 sigma) was
44 4.8×10^5 molecules cm^{-3} ."

45 page 10 line 21-23: "The uncertainty of the calculated missing source S_{HONO} was estimated to be about 16%,
46 based on the Gaussian error propagation of instrument uncertainties of HONO, NO, NO₂, J, and OH."

1 in Fig. 5a/b error bars based on standard deviation of diel mean values are added



2
3 Revised Fig. 5a+b including error bars; as suggested in another comment, the NO₂ conversion rate for the
4 heterogeneous reaction in the dry case (b) is now adopted as suggested by the referee. (ΔHONO/Δt was added as
5 discussed in a comment by reviewer 2)
6

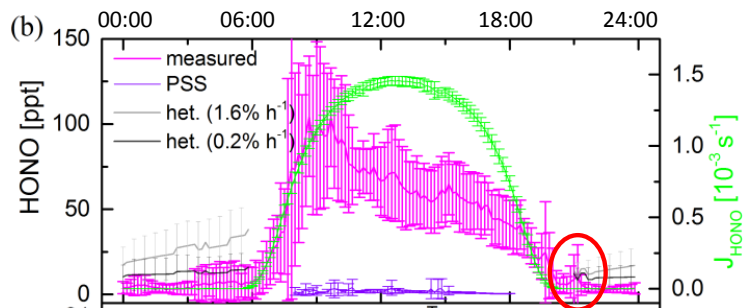
7 **Specific comment:**

8 *In section 5.1, the heterogeneous reaction of NO₂ to form HONO is estimated by applying an NO₂-HONO*
9 *conversion rate of 1.6% h⁻¹ overnight. Under humid conditions the estimated values agree well with measured*
10 *values. A much lower rate of 0.22 % h⁻¹ was applied in the drier period, which the author's state matches better to*
11 *their observations. However, Fig 4. shows the measured HONO is still lower than the estimated values during some*
12 *periods overnight. Perhaps it would be better to determine a conversion rate under dry conditions for this site using*
13 *the NO_x scaling approach (e.g. Sorgel et al., 2011) to compare with other studies, as I expect it is lower.*

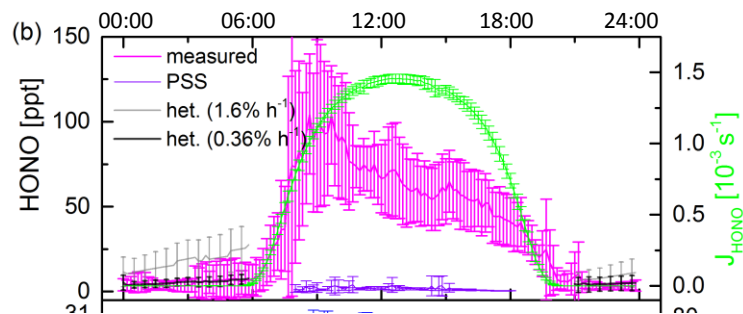
14 **Response:**

15 Thank you for this comment and suggestion. Accordingly, we now use the approach from Alicke et al.,
16 2002+2003; Su et al. 2008b and Sörgel et al., 2011b for the conversion rate of the dry nights: $rate =$
17 $\frac{HONO_{t2} - HONO_{t1}}{\Delta t + NO_2}$. The respective average conversion rate is now 0.36% h⁻¹ (slightly higher than the 0.22 % h⁻¹ used
18 before).

19 Also, a more representative HONO nighttime starting concentration 4.4 ppt is now used to better match the
20 observations (as the original starting concentration 12.2 ppt was too high, the observed average concentration
21 decreased afterwards, see marked area in old fig 4b).
22



23 Upper panel of old Fig. 4b,
24



1 Upper panel of revised Fig. 4b with adopted nighttime NO_2 conversion rate based on Soergel et al. (2011b) and a
 2 more representative HONO nighttime starting concentration. According to comment below, error bars are now in
 3 darker color.
 4
 5

6 The manuscript, section “5.1 nighttime HONO accumulation” on page 8 from line 15-33 is now revised to:
 7 “Instead, nighttime HONO concentrations can be estimated due to heterogeneous reaction of NO_2 described in
 8 Eq. (1) (Alicke et al., 2002+ 2003; Su et al., 2008b; Sörgel et al., 2011b). Three studies in different environments
 9 from a rural forest region in East Germany (Sörgel et al., 2011b) and a non-urban site in the Pearl River delta,
 10 China (Su et al., 2008b) to an urban, polluted site in Beijing (Spataro et al., 2013) found a conversion rate of
 11 about $1.6\% \text{ h}^{-1}$ ($1.1\text{-}1.8\% \text{ h}^{-1}$).

$$12 \quad [\text{HONO}]_{\text{het}} = [\text{HONO}]_{\text{evening}} + 0.016 \text{ h}^{-1} [\text{NO}_2] \Delta t, \quad (\text{Eq. 1})$$

13 $[\text{HONO}]_{\text{het}}$ denotes the accumulation of HONO by heterogeneous conversion of NO_2 , $[\text{HONO}]_{\text{evening}}$ the
 14 measured HONO mixing ratio at 20:30 LT, $[\text{NO}_2]$ the measured average NO_2 mixing ratio between 20:30 and
 15 7:30 LT, Δt time span in hours.

16 Measured and calculated HONO mixing ratios are compared in figure 4 (upper panel). During the humid period,
 17 during night the estimated (according Eq. (1), fig. 4a upper panel, grey line) and observed HONO mixing ratios
 18 are in good agreement ($R^2 = 0.9$). During the drier period the observed HONO mixing ratios were lower than the
 19 ones calculated with a NO_2 conversion rate of $1.6\% \text{ h}^{-1}$. **Here the approach for the nighttime conversion**
 20 **frequency by e.g. Alicke et al., 2002+2003, Su et al., 2008b or Sörgel et al., 2011b (rate = $\frac{\text{HONO}_{t2} - \text{HONO}_{t1}}{\Delta t + \text{NO}_2}$) was**
 21 **used. The 7 days average conversion rate for the dry nights was $0.36\% \text{ h}^{-1}$ (fig. 4b, upper panel, black line),**
 22 **comparable to results of Kleffmann et al. (2003) reporting a conversion rate of $6 \times 10^{-7} \text{ s}^{-1}$ ($0.22\% \text{ h}^{-1}$) for rural**
 23 **forested land in Germany.”**

24 **comments:**

25
 26 Pg 3, L25-26. Please state the uncertainty of the HONO measurements here too.

27 See comment above, the HONO uncertainty is now stated in this section.

28
 29 Pg 6, L18. The \pm values in the parenthesis should be clarified. Are these 1-sigma standard deviation of the mean?

30 Correct, this is now declared in the text on page 6 line 25: “...(± 25 pptv, 1σ standard deviation, following alike)”

31
 32 Pg 7, L7. It is stated that the mean NO mixing ratios are close to the detection limit at 2 pptv, however, this is
 33 actually below the detection limit, which is given as 5 pptv on Pg 4, L13.

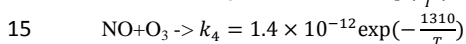
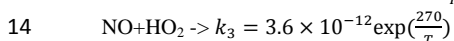
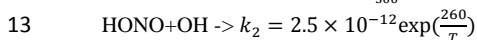
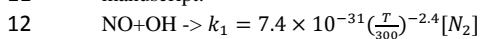
34 Sorry for this typo. Now the correct detection limit of 5 pptv of NO as written in the instrument description is
 35 now used here.
 36

1 Pg 8, L5-7. Here, HONO mixing ratios are estimated and compared to the measured HONO overnight using a
2 conversion factor between NO₂ and HONO of 1.6% h⁻¹. The authors cite three studies where this value has been
3 determined, although, it should be made clear here that a range of values were reported across these studies.

4 Correct. Now the range of values is stated in the modified version (see response on comment above) Sörgel et al.
5 (2011) reported 1.1 (±0.65) % h⁻¹, Spataro et al. (2013) 1.5-1.8 % h⁻¹ and Su et al. (2008) came up with a best
6 estimate of 1.6 % h⁻¹, based on different scaling methods.
7

8 Pg 9, L25. Please state the values for k₁ and k₂ used in Eq. 2.

9 The rate constants k₁, k₂ (and k₃ and k₄) are temperature dependent, so stating only one value would not be
10 appropriate. The respective formulas were taken from Atkinson et al. (2004), as was already cited in the original
11 manuscript.



16 E.g. at a temperature of 23°C, typical for the measurement time on Cyprus: k₁ = 1.36x10⁻¹¹ s⁻¹, k₂ = 6.01x10⁻¹² s⁻¹,
17 k₃ = 8.96x10⁻¹² s⁻¹, k₄ = 1.68x10⁻¹⁴ s⁻¹

18 In the revised manuscript the temperature dependence is now pointed out, and respective numbers are given for a
19 typical daytime temperature on Cyprus during the campaign (23°C)
20

21 Fig 4: The error bars in figure 4b for the 0.2% rate are difficult to see, please use a darker color or use thicker lines.

22 Thanks for indicating. Fig 4b is now changed accordingly (see response on comment above).
23

24 In Figure 5, the caption states that a conversion rate of 1.6% h⁻¹ is used for S_{Het,NO₂}, however, Figure 4b shows that
25 a lower rate (0.22% h⁻¹) is more appropriate for the dry period. Please clarify which rate you use for Fig 5b.

26 Correct. Indeed, in the original manuscript 1.6% h⁻¹ was used for both by mistake. In the revised manuscript the
27 conversion rate adopted by Soergel et al. (2011b) is now used (0.36% h⁻¹; see comment above), and the figure
28 caption corrected accordingly. We thank the reviewer for exposing this critical detail.
29

30 Fig 6. Include units for NO₂ in the legend.

31 Thanks, has been corrected accordingly.
32

33 Fig. 4 and Fig 7. Please state in the figure captions what the error bars represent.

34 The error bars represent one standard deviation of diel mean values. This is now specified in the figure captions
35 of the revised manuscript (Fig. 4 and 7).
36
37

38 References

39 Sörgel, M., Trebs, I., Serafimovich, A., Moravek, A., Held, A., and Zetzsch, C.: Simultaneous HONO measurements
40 in and above a forest canopy: influence of turbulent exchange on mixing ratio differences, Atmos. Chem. Phys., 11,
41 841-855, 2011(b)

42 Alicke, B., Platt, U., Stutz, J.: Impact of nitrous acid photolysis on the total hydroxyl radical budget during the
43 limitation of oxidant production/pianura padana produzione di ozono study in Milan. Journal of Geophysical
44 Research 107 (D22), 8196, 2002.
45

- 1 Alicke, B., Geyer, A., Hofzumahaus, A., Holland, F., Konrad, S., Paetz, H.W., Schaefer, J., Stutz, J., Volz-Thomas,
2 A., Platt, U.: OH formation by HONO photolysis during the BERLIOZ experiment. Journal of Geophysical Research
3 108 (D4), 8247, 2003.
4
- 5 Atkinson, R., Baulch, D. L., Cox, R. A., Crowley, J. N., Hampson, R. F., Hynes, R. G., Jenkin, M. E., Rossi, M. J.,
6 and Troe, J.: Evaluated kinetic and photochemical data for atmospheric chemistry: Volume I - gas phase reactions of
7 O-x, HOx, NOx and SOx species, Atmospheric Chemistry and Physics, 4, 1461-1738, 2004.
8
- 9 Su, H., Cheng, Y. F., Cheng, P., Zhang, Y. H., Dong, S., Zeng, L. M., Wang, X., Slanina, J., Shao, M., and
10 Wiedensohler, A.: Observation of nighttime nitrous acid (HONO) formation at a non-urban site during PRIDE-
11 PRD2004 in China, Atmospheric Environment, 42, 6219-6232, 2008(b).
12
- 13 Spataro, F., Ianniello, A., Esposito, G., Allegrini, I., Zhu, T., and Hu, M.: Occurrence of atmospheric nitrous acid in
14 the urban area of Beijing (China), The Science of the total environment, 447, 210-224, 2013.
15
16

17 **Anonymous Referee #2**

19 **General comments:**

20 *This paper uses measurements of HONO with a wide range of supporting data to assess sources of HONO in the*
21 *remote coastal site in Cyprus. The findings are that there is a common source of HONO and NO and it is speculated*
22 *that this is emission from microbial communities on soil surfaces. The work is important as HONO provides a route*
23 *to OH radicals that is often not considered and sources of HONO in both urban and remote regions are uncertain.*
24 *The authors have done a good job presenting their data and the conclusions they draw are reasonable. It*
25 *undoubtedly adds to the sphere of knowledge surrounding atmospheric HONO. The paper is well presented with*
26 *good clear figures and should be published in ACP subject to the authors addressing the following comments.*

27 **Response:**

28 We thank the reviewer for the positive feedback. Please find our point-to-point responses listed below.
29

30 **Specific comment:**

31 *The main conclusion of the paper is that there is a soil source of HONO and NO, which is arrived upon by looking at*
32 *correlations between the 'missing' HONO source (i.e. the difference between HONO calculated using a steady state*
33 *approximation including a series of known sources and the measured HONO) and a missing source of NO (based on*
34 *NO deviations from the Leighton ratio). A strong correlation is given as evidence of a common source. Is this source*
35 *thought to be photolytically driven? If not why are observations of NO at night seemingly zero (although it is quite*
36 *difficult to see the exact levels on the plots), whereas HONO is shown to increase during the night. Maybe this is just*
37 *a result of NO reacting with O₃ before the measurement location but the authors should clarify this.*

38 **Response:**

39 True, the correlation analysis was based on daytime values only. For nighttime conditions, the chemistry is
40 relatively slow and transport processes could strongly influence the budget of nitrogen-containing species, that's
41 why we focus on the daytime chemistry.
42 The difference in nighttime accumulation of NO and HONO may be due to other reasons, like NO₂
43 heterogeneous conversion, being relevant for HONO accumulation within a shallow nocturnal boundary layer
44 (here 0.4-1.6 %, in line with other literature, see chapter "5.1 nighttime HONO accumulation"), while there is no
45 chemical source for NO. Also the nighttime reaction of NO + OH forming HONO would result in a preference in
46 HONO accumulation, with nighttime OH concentration sometimes as high as 1x10⁶ molecules cm⁻³ (see Fig. S3).

1 As suggested by the referee, NO titration by the reaction with O₃ may also play a role for the absence of
2 nighttime NO accumulation, with continuously high O₃ concentrations (60-90 ppb), while there is no major loss
3 of HONO due to the lack of photolysis. Another option would be different temperature dependencies of NO and
4 HONO emissions from soil (e.g., Oikawa et al., 2015; Mamtimin et al., 2016, which is now stated on page 12 line
5 31-35).

6 We modified one sentence of the “result” chapter, page 7, line 22). “In the absence of local NO sources low
7 nighttime values are a result of the conversion of NO to NO₂ by O₃ which was continuously high (Beygi et al.,
8 2011)”
9

10 **Specific comment:**

11 *How far from the potential soil emission source in the measurement site? The authors should also comment on how*
12 *this effects the validity of the steady state approximation, with reference to the Lee et al. 2013 study that gives*
13 *caveats for the use of a steady state approximation to interpret HONO measurements.*

14 **Response:**

15 Thanks to the comment. We are afraid that we may not have described our calculation properly and the using of
16 HONO_{PPS} was misleading. We actually followed the method in Su et al. (2008a) to calculate HONO missing
17 source. With this method, we did not assume HONO to be at PSS, because the measured d[HONO]/dt has been
18 accounted in the HONO missing source estimation and according to our measurement d[HONO]/dt was not equal
19 to zero, which did mean that HONO was not at PSS.

$$20 S_{\text{HONO}} = J_{\text{HONO}}[\text{HONO}] + k_2[\text{OH}][\text{HONO}] - k_1[\text{OH}][\text{NO}] - k_{\text{het}}[\text{NO}_2] + \frac{\Delta[\text{HONO}]}{\Delta t}$$

21 Lee et al. (2013) states that assuming HONO to be completely at PSS will likely overestimate the strength of any
22 “unknown source”. In the Lee et al. (2013) case, the authors would come up with up to 1.1 ppb h⁻¹ with the PSS
23 approach. They argue that instead of presuming a PSS, they can explain the observed HONO from pure precursor
24 chemistry by applying a simple chemical box model.

25 Lee et al. (2013) argue that the PSS assumption might not have been valid for their case study, because the
26 transport time from nearby NO_x vehicle exhaust emission sources to the measurement site was likely less than the
27 time required for HONO to reach PSS. Using a chemical box model, Lee et al. (2013) demonstrated that there is
28 initially net HONO formation from assumed strong emissions (100 ppm for the sum of NO, NO₂, HONO), as
29 high levels of NO in vehicle exhaust react with assumed entrainment of ambient OH. In the respective model
30 daytime show-case, this HONO net production (d[HONO]/dt>0), sustained for 2.5 min after precursor emission.
31 Subsequently, net HONO loss dominated by photolysis led to a negative d[HONO]/dt in their calculations, which
32 was sustained for several minutes until PSS is established after ca. 10 min (for mean daytime conditions) or up to
33 several hours depending on time of day. This way, Lee et al. (2013) claim that “for all conditions, d[HONO]/dt is
34 negative for a specific period of time, during which sampling vehicle exhaust can lead to overestimates of
35 secondary HONO sources *if a photostationary state is inappropriately assumed*”, and hence “... there exists a
36 window of time in which d[HONO]/dt is negative. Erroneously assuming the presence of PSS during this time
37 period would lead to overestimates of secondary HONO sources.”

38 With respect to our analysis, first of all, we did not assume that HONO PSS is fully established at our
39 measurement site (d[HONO]/dt was not equal to 0). However, even though for the Cyprus case, the mean upwind
40 distance between the measurement site and the coast line is about 6 km. With a mean wind velocity of 3 m s⁻¹ the
41 respective air mass travel time over land/soil surface is about half an hour, i.e., several times the daytime lifetime
42 of HONO. Moreover, and in strong contrast to Lee et al. (2013), at the Cyprus site the concentrations of HONO
43 precursors were extremely low. In the Cyprus case, the observed atmospheric load of precursors (NO and OH) is
44 by far too low to explain the observed HONO concentrations, or d[HONO]/dt, respectively (see Fig. 5). Even
45 doubling the contribution of the chemical source (NO + OH) would not lead to a substantial reduction of the
46 strength of the calculated un-identified HONO source.

47 To account for any caveats of any PSS assumptions, we now state in the text (page 10, line 14-30):

“Lee et al. (2013) argue that the HONO PSS assumption might overestimate the strength of any un-identified source, if the transport time from nearby NO_x emission sources to the measurement site is less than the time required for HONO to reach PSS. In this study, the missing source was calculated according to Su et al., 2008a (eq.3), where PSS was not assumed. Also in our measurements, dHONO/dt was not equal to zero, as HONO was not at PSS.

$$S_{\text{HONO}} = J_{\text{HONO}}[\text{HONO}] + k_2[\text{OH}][\text{HONO}] - k_1[\text{OH}][\text{NO}] - k_{\text{het}}[\text{NO}_2] + \frac{\Delta[\text{HONO}]}{\Delta t} \quad (\text{Eq.3})$$

with [HONO] being the measured HONO concentration and k_{het} the heterogeneous conversion rate of NO₂ to HONO, which was discussed above to be 1.6% h⁻¹ during the wet period and 0.36% h⁻¹ during the dry period. Δ[HONO]/Δt is the observed change of HONO concentration unequal to 0. The uncertainty of the calculated missing source S_{HONO} was estimated to be about 16% based on the Gaussian error propagation of instrument uncertainties of HONO, NO, NO₂, J and OH.

Nevertheless, at the study site of Cyprus, the mean upwind distance between the measurement site and the coast line was about 6 km, and the mean wind velocity was about 3 m s⁻¹. Accordingly, the respective air mass travel time over land is estimated to be about half an hour, which is somewhat longer than the daytime lifetime of HONO and might provide enough time for the equilibrium processes. Furthermore and in a strong contrast to Lee et al. (2013), at the Cyprus site the concentrations of HONO precursors (NO and OH) were extremely low, by far too low to explain the observed HONO concentrations.“

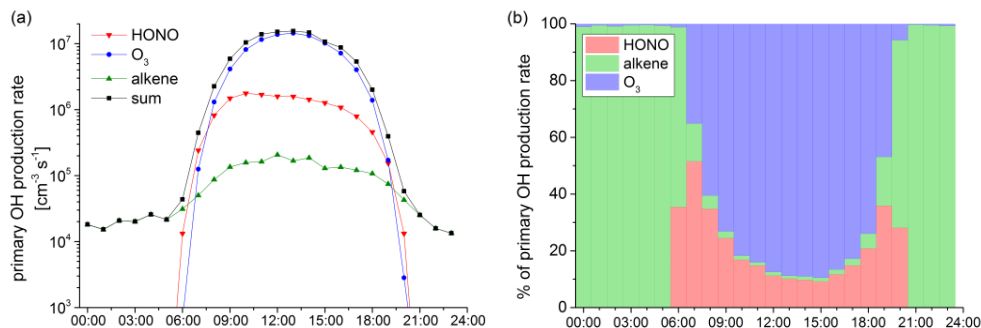
Specific Comment:

I find the analysis of OH production showing the importance of HONO confusing because it details production of OH from HCHO, which is indirect and requires conversion of the HO₂ produced with NO to form OH. I believe it would be better to just include HO₂ + NO as an OH source, regardless of where the HO₂ is coming from. Another option would be to have a total HO_x radical budget analysis.

Response:

We thank the referee for disclosing this critical detail. OH budget analysis including photolysis of HCHO was done before e.g. by Alicke et al., 2002 but then also RO₂ primary production should be considered as it will also be converted in OH through cycling processes. HONO photolysis, ozonolysis of alkenes and photolysis of O₃ and subsequent reaction with water contribute to the primary OH production. HCHO photolysis firstly forms HO₂ which is in fast equilibrium with OH e.g. via the reaction of HO₂ and NO. Therefore it contributes to secondary OH production. In this study we focus on the evaluation of HONO sources and wanted to give a brief outlook on its importance on OH. To realize this we just show the primary OH production routes (and deleted the OH production via HCHO photolysis). Furthermore we changed the term “OH production” into “primary OH production”.

As written below, a complete detailed HO_x budget analysis will be published from colleagues soon.



Revised fig. 9: Average diel pattern of primary OH production from HONO, O₃ and VOC, shown as a) production rate and b) percentage contributions to primary OH production.

1
2 **Specific Comment:**
3 *The authors should also comment on the fact that the HONO source here is only important near to the surface (an*
4 *estimate could be made of the vertical structure of HONO) and thus it is not relevant for the entire troposphere. This*
5 *is important when considering HONO as an atmospheric 'oxidant'.*

6 **Response:**
7 Indeed, many studies have shown decreasing HONO mixing ratios with altitude in the lowest few hundred meters
8 of the troposphere (Vogel et al., 2003; Zhang et al., 2009; Young et al., 2012; Wong et al., 2012 and 2013;
9 VandenBoer et al., 2013). According to the modelling results of Wong et al. 2013, we estimate that the ground
10 HONO source could be important for up to 200–300 m a.g.l. According to the referee's suggestion we now state
11 in the introduction (Page 3, line 9-13):
12 "Many studies have shown decreasing HONO mixing ratios with altitude in the lowest few hundred meters of the
13 troposphere, due to respective short atmospheric lifetime compared to vertical transport time (Wong et al., 2012
14 and 2013; Vogel et al., 2003; VandenBoer et al., 2013; Zhang et al., 2009; Young et al., 2012;). According to the
15 modelling results of Wong et al. 2013, we estimate that the ground HONO source could be important for up to
16 200–300 m a.g.l. This indicates that HONO is more relevant for the OH budget close to the surface than in high
17 altitude air masses."
18

19 **Comment:**
20 *The authors mention in the experimental description that OH was measured during the field campaign but there is*
21 *then no further mention of it in the manuscript. Have the authors (or anyone else) examined the OH data to assess if*
22 *the measured HONO is required to close the HO_x budget? I realise this may be the subject of further publications*
23 *but if it is stated that HO_x was measured it seems odd that no mention is made of the results.*

24 **Response:**
25 We thank the referee for this suggestion. In this study, we focused on HONO and its missing daytime source. OH
26 data were used to calculate the HONO budget and HO₂ data were used to study the NO budget. The potential
27 contribution of HONO photolysis to OH production is studied in a short chapter showing different OH production
28 routes. A "total HO_x radical budget analysis" is not focus of this manuscript. A future CYPHEX paper of
29 colleagues will deal with the HO_x budget closure study, including a detailed box modelling approach for the total
30 HO_x budget and OH recycling. The manuscript will be submitted soon.
31

32 **Comment:**
33 *The manuscript is generally well referenced however a recent study by Lee et al. 2016 in London contains a lot of*
34 *detail about potential HONO sources in an urban area and should be referenced. There is also a recent study by*
35 *Mamtimin et al. (2016) which discusses biogenic NO and HONO emissions that seems to be extremely relevant to*
36 *this work. The authors should comment on how their results compare to this.*

37 **Response:**
38 We greatly appreciate these reference suggestions. Both fit well into this study.
39 Mamtimin et al., 2016 is now cited in the introduction (page 3, line3), and twice in "common daytime source of
40 HONO and NO" (page 12, line 28 and line 31-35) when comparing with other studies on HONO and NO emission.
41 "Mamtimin et al. (2016) investigated HONO and NO emissions of natural desert soil and with grapes or cotton
42 cultivated soils in an oasis in the Taklamakan desert in the Xinjiang region in China. After irrigation they didn't
43 find direct emission, but when the soil had almost dried out (gravimetric soil water content 0.01-0.3) emissions up
44 to 115 ng N m⁻² s⁻¹ were detected. In addition they observed soil-temperature dependent emission of reactive
45 nitrogen.
46 Lee et al. (2016) is now cited once in the introduction (page 3, line 17) and in "daytime HONO budget" (page 11,
47 line 15-16), discussing possible light induced HONO formation and comparing correlation factors:

1 “Lee et al. (2016) found even lower correlation with [NO₂] (R² = 0.0001) but similar good correlation with
2 J_{NO₂}*[NO₂] (R²=0.70) at an urban background site in London.”

3
4
5 **Minor comments:**

6 *The authors should make sure they clarify what the error bars on plots and in the text actually refer to (e.g. figures 4*
7 *and 7)*

8 Correct. As also suggested by Referee #1, we now clarify what the error bars on plots and in the text actually
9 refer to. Error bars in Fig. 4 and 7 (and ± values) indicate standard deviation (1 sigma).

10
11 *P. 12 line 11: Use O₃ rather than ozone as has been done in the rest of the manuscript*

12 Thanks for noticing. Is now changed accordingly in the text.

13
14 *P. 7 line 7: there is a discrepancy between the detection limit stated here (2pptv) and that in the experimental section*
15 *(5pptv) – please confirm.*

16 Thanks for indicating. As also suggested by referee #1, a detection limit of 5 pptv is now stated in the revised
17 versions of the manuscript.

18

19 **References:**

20 Mamtimin, B., Meixner, F. X., Behrendt, T., Badawy, M., and Wagner, T.: The contribution of soil biogenic NO and
21 HONO emissions from a managed hyperarid ecosystem to the regional NO_x emissions during growing season,
22 Atmos. Chem. Phys., 16, 10175-10194, 2016.

23
24 Lee, J. D., Whalley, L. K., Heard, D. E., Stone, D., Dunmore, R. E., Hamilton, J. F., Young, D. E., Allan, J. D.,
25 Laufs, S., and Kleffmann, J.: Detailed budget analysis of HONO in central London reveals a missing daytime source,
26 Atmos. Chem. Phys., 16, 2747-2764, 2016.

27
28 Lee, B. H., Wood, E. C., Herndon, S. C., Lefer, B. L., Luke, W. T., Brune, W. H., Nelson, D. D., Zahniser, M. S.,
29 and Munger, J. W.: Urban measurements of atmospheric nitrous acid: A caveat on the interpretation of the HONO
30 photostationary state, J. Geophys. Res., vol. 118, 12274–12281, 2013.

31
32 Oikawa, P. Y., Ge, C., Wang, J., Eberwein, J. R., Liang, L. L., Allsman, L. A., Grantz, D. A., and Jenerette, G. D.:
33 Unusually high soil nitrogen oxide emissions influence air quality in a high-temperature agricultural region, Nat.
34 Commun., 6, 2015.

35

36 Alicke, B., Platt, U., Stutz, J.: Impact of nitrous acid photolysis on the total hydroxyl radical budget during the
37 limitation of oxidant production/pianura padana produzione di ozono study in Milan. Journal of Geophysical
38 Research 107 (D22), 8196, 2002.

39
40 Vogel, B., Vogel, H., Kleffmann, J., and Kurtenbach, R.: Measured and simulated vertical profiles of nitrous acid -
41 Part II. Model simulations and indications for a photolytic source, Atmospheric Environment, 37, 2957-2966, 2003.

42
43 VandenBoer, T. C., Brown, S. S., Murphy, J. G., Keene, W. C., Young, C. J., Pszenny, A. A. P., Kim, S., Warneke,
44 C., de Gouw, J. A., Maben, J. R., Wagner, N. L., Riedel, T. P., Thornton, J. A., Wolfe, D. E., Dubé, W. P., Öztürk,
45 F., Brock, C. A., Grossberg, N., Lefer, B., Lerner, B., Middlebrook, A. M., and Roberts, J. M.: Understanding the

1 role of the ground surface in HONO vertical structure: High resolution vertical profiles during NACHTT-11, Journal
2 of Geophysical Research: Atmospheres, 118, 10,155-110,171, 2013.
3
4 Wong, K. W., Tsai, C., Lefer, B., Haman, C., Grossberg, N., Brune, W. H., Ren, X., Luke, W., and Stutz, J.: Daytime
5 HONO vertical gradients during SHARP 2009 in Houston, TX, Atmospheric Chemistry and Physics, 12, 635-652,
6 2012.
7
8 Wong, K. W., Tsai, C., Lefer, B., Grossberg, N., and Stutz, J.: Modeling of daytime HONO vertical gradients during
9 SHARP 2009, Atmospheric Chemistry and Physics, 13, 3587-3601, 2013.
10
11 Young, C. J., Washenfelder, R. A., Roberts, J. M., Mielke, L. H., Osthoff, H. D., Tsai, C., Pikelnaya, O., Stutz, J.,
12 Veres, P. R., Cochran, A. K., VandenBoer, T. C., Flynn, J., Grossberg, N., Haman, C. L., Lefer, B., Stark, H., Graus,
13 M., de Gouw, J., Gilman, J. B., Kuster, W. C., and Brown, S. S.: Vertically Resolved Measurements of Nighttime
14 Radical Reservoirs; in Los Angeles and Their Contribution to the Urban Radical Budget, Environmental Science &
15 Technology, 46, 10965-10973, 2012.
16
17 Zhang, N., Zhou, X. L., Shepson, P. B., Gao, H. L., Alaghmand, M., and Stirm, B.: Aircraft measurement of HONO
18 vertical profiles over a forested region, Geophysical Research Letters, 36, 2009.
19
20
21

1 Daytime formation of nitrous acid at a coastal remote site in 2 Cyprus indicating a common ground source of atmospheric 3 HONO and NO

4 Hannah Meusel, Uwe Kuhn¹, Andreas Reiffs², Chinmay Mallik², Hartwig Harder², Monica
5 Martinez², Jan Schuladen², Birger Bohn³, Uwe Parchatka², John N. Crowley², Horst Fischer²,
6 Laura Tomsche^{2,3}, Anna Novelli^{2,3}, Thorsten Hoffmann⁴, Ruud Janssen^{2,5}, Oscar Hartogensis^{5,6},
7 Michael Pikridas^{7,6}, Mihalis Vrekoussis^{6,7,8,9}, Efstratios Bourtsoukidis², Bettina Weber¹, Jos
8 Lelieveld², Jonathan Williams², Ulrich Pöschl¹, Yafang Cheng¹, Hang Su¹

9 ¹Max Planck institute for Chemistry, Multiphase Chemistry Department, Mainz, Germany

10 ²Max Planck Institute for Chemistry, Atmospheric Chemistry Department, Mainz, Germany

11 ³Institute for Energy and Climate Research (IEK-8), Research Center Jülich, Jülich, Germany

12 ⁴Johannes Gutenberg University, Inorganic and Analytical Chemistry, Mainz, Germany

13 ⁵MeteoGroup, Wageningen, Netherlands

14 ⁶Wageningen University and Research Center, Meteorology and Air Quality, Wageningen, Netherlands

15 ⁶²Cyprus Institute, Energy, Environment and Water Research Center, Nicosia, Cyprus

16 ⁷⁸Institute of Environmental Physics and Remote Sensing – IUP, University of Bremen, Germany

17 ⁸⁹Center of Marine Environmental Sciences – MARUM, University of Bremen, Germany

18 Correspondence to: Hang Su (h.su@mpic.de)

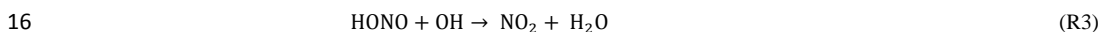
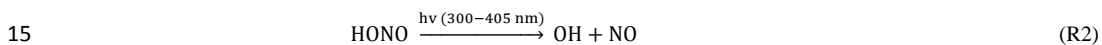
19 **Abstract.** Characterization of daytime sources of nitrous acid (HONO) is crucial to understand atmospheric
20 oxidation and radical cycling in the planetary boundary layer. HONO and numerous other atmospheric trace
21 constituents were measured on the Mediterranean island of Cyprus during the CYPHEX campaign (CYPHEX =
22 Cyprus PHotochemical EXperiment) in summer 2014. Average volume mixing ratios of HONO were 35 pptv (± 25
23 pptv) with a HONO/NO_x ratio of 0.33, which was considerably higher than reported for most other rural and urban
24 regions. Diel profiles of HONO showed peak values in the late morning (60 \pm 28 pptv around 09:00 local time), and
25 persistently high mixing ratios during daytime (45 \pm 18 pptv) indicating that the photolytic loss of HONO is
26 compensated by a strong daytime source. Budget analyses revealed unidentified sources producing up to 3.4 x 10⁶
27 molecules cm⁻³ s⁻¹ of HONO and up to 2.0 x 10⁷ molecules cm⁻³ s⁻¹ NO. Under humid conditions (RH >70%), the
28 source strengths of HONO and NO exhibited a close linear correlation (R²=0.782), suggesting a common source that
29 may be attributable to emissions from microbial communities on soil surfaces.

30 1 Introduction

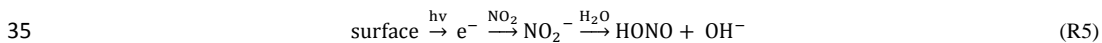
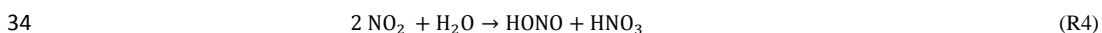
31 Nitrous acid (HONO) is an important component of the nitrogen cycle being widely spread in the environment.
32 Either in its protonated form (HONO or HNO₂) or as nitrite ions (NO₂⁻) it can be found in the gas phase, on aerosol-
33 particles, in clouds and dew droplets but also in soil, sea-water and sediments (Foster et al., 1990; Rubio et al., 2002;
34 Acker et al., 2005 and 2008; Bianchi et al., 1997). It plays a key role in the oxidizing capacity of the atmosphere, as
35 it is an important precursor of the OH radical, which initiates most atmospheric oxidations. OH radicals react with
36 pollutants in the atmosphere to form mostly less toxic compounds (e.g. CO + OH → CO₂ + H₂O; Levy, 1971).
37 Volatile organic compounds (VOCs) react with OH contributing to formation of secondary aerosols (SOA), which

1 can serve as cloud condensation nuclei CCN (Arey et al., 1990; Duplissy et al., 2008). Furthermore OH oxidizes SO₂
 2 to H₂SO₄, which condense subsequently to form aerosol particles (Zhou et al. 2013). In this way HONO has an
 3 indirect effect on the radiative budget and climate. In the first 2-3 hours following sunrise, when OH production from
 4 other sources (photolysis of O₃ and formaldehyde) is relatively low, photolysis of HONO can be the major source of
 5 OH radicals as HONO concentrations may be high after accumulation during night time (Lammel and Cape, 1996;
 6 Czader et al., 2012; Mao et al., 2010). On average up to 30% of the daily OH budget in the boundary layer is
 7 provided by HONO photolysis (Alicke et al., 2002; Kleffmann et al., 2005; Ren et al., 2006), but has been reported
 8 as high as 56% (Ren et al., 2003) with ambient HONO mixing ratios ranging from several pptv in rural areas up to a
 9 few ppb in highly polluted regions (Acker et al., 2006a and 2006b; Costabile et al., 2010; Li et al., 2012; Michoud et
 10 al., 2014; Spataro et al., 2013; Su et al. 2008a; Zhou et al., 2002a).

11 In early studies, atmospheric HONO was assumed to be in a photostationary state during daytime controlled by the
 12 gas phase reaction of NO and OH (R1) and two loss reactions which are the photolysis (R2) and the reaction with
 13 OH (R3).



17 However, field measurements in remote and rural locations, as well as urban and polluted regions found several
 18 times higher daytime HONO concentrations than model predictions, suggesting a large unknown source (Kleffmann
 19 et al., 2003 and 2005; Su et al., 2008a; Soergel et al., 2011a; Su et al., 2011; Michoud et al., 2014; Czader et al.,
 20 2012; Wong et al., 2013; Tang et al., 2015; Oswald et al., 2015) even after considering direct emission of HONO
 21 from combustion sources (Kessler and Platt, 1984; Kurtenbach et al., 2001). Heterogeneous reactions on aerosols
 22 have been proposed as an explanation for the missing source. The hydrolysis (R4, Finlayson-Pitts et al., 2003) and
 23 redox reactions of NO₂ have been intensively investigated on different kinds of surfaces such as fresh soot, aged or
 24 organic-coated particles (Ammann et al., 1998; Arens et al., 2001; Aubin et al., 2007; Bröske et al., 2003; Han et al.,
 25 2013; Kalberer et al., 1999; Kleffmann et al., 1999; Kleffmann and Wiesen, 2005; Lelievre et al., 2004). Minerals
 26 like SiO₂, CaCO₃, CaO, Al₂O₃, and Fe₂O₃ showed a catalytic effect on the hydrolysis of NO₂ (Kinugawa et al., 2011;
 27 Liu et al., 2015; Wang et al., 2003; Yabushita et al., 2009). Different kind of surfaces (humic acid and other organic
 28 compounds, titanium dioxide, soot) can be photochemically activated which leads to enhanced NO₂ uptake and
 29 HONO production (R5, George et al., 2005; Langridge et al., 2009; Monge et al., 2010; Ndour et al., 2008; Ramazan
 30 et al., 2004; Stemmler et al., 2007; Kebede et al., 2013). The photolysis of particulate nitric acid (HNO₃), nitrate
 31 (NO₃⁻) and nitro-phenols (R-NO₂) lead to HONO formation as well (Baergen and Donaldson, 2013; Bejan et al.,
 32 2006; Ramazan et al., 2004; Scharko et al., 2014; Zhou et al., 2003; Zhou et al., 2011). But these reactions cannot
 33 account for the HONO levels observed during daytime (Elshorbany et al., 2012).



1 On the other hand, soil nitrite, either biogenic or non-biogenic, has been suggested as an effective source of HONO
2 (Su et al., 2011; Oswald et al., 2013; Mamtimin et al., 2016). Depending on soil properties such as pH and water
3 content and according to Henry's law HONO can be released (Donaldson et al., 2014b; Su et al., 2011). This is
4 consistent with field flux measurements showing HONO emission from the ground rather than deposition as is the
5 case for HNO₃ (Harrison and Kitto, 1994; Kleffmann et al., 2003; Ren et al., 2011; Stutz et al., 2002; VandenBoer et
6 al., 2013; Villena et al., 2011; ~~Wong et al., 2012 and 2013~~; Zhou et al., 2011). In a recent study, Weber et al. (2015)
7 measured large HONO- and NO-emissions from dryland soils with microbial surface communities (so-called
8 biological soil crusts). Many studies have shown decreasing HONO mixing ratios with altitude in the lowest few
9 hundred meters of the troposphere, due to respective short atmospheric lifetime compared to vertical transport time
10 (Wong et al., 2012 and 2013; Vogel et al., 2003; VandenBoer et al., 2013; Zhang et al., 2009; Young et al., 2012).
11 According to the modelling results of Wong et al. 2013, we estimate that the ground HONO source could be
12 important for up to 200–300 m a.g.l. This indicates that HONO is more relevant for the OH budget close to the
13 surface than in high altitude air masses.

14 Several field studies also show a correlation of the unknown HONO source with solar radiation or the photolysis
15 frequency of NO₂ J_{NO2} (Su et al., 2008a; Söörger et al., 2011a; Wong et al., 2012; Costabile et al., 2010; Michoud et
16 al., 2014; Oswald et al., 2015; Lee et al., 2016). This correlation can be explained either by the aforementioned
17 photosensitized reactions or by temperature-dependent soil-atmosphere exchange (Su et al., 2011). According to Su
18 et al. (2011), the release of HONO from soil surfaces is controlled by both the soil (biogenic and chemical)
19 production of nitrite and the gas-liquid phase equilibrium. The solubility is strongly temperature-dependent, resulting
20 in a higher HONO emission during noon time and high radiation J_{NO2} periods, and lower HONO emissions or even
21 HONO deposition during the nighttime as further confirmed by VandenBoer et al. (2015). This temperature
22 dependence not only exists for equilibrium over soil solution but also exists for adsorption/desorption equilibrium
23 over dry and humid soil surfaces (Li et al., 2016).

24 In this study we measured HONO and a suite of other atmospherically relevant trace gases in a coastal area on the
25 Mediterranean Island Cyprus in summer 2014. Due to low local anthropogenic impact and low NO_x levels in aged
26 air masses, but high solar radiation, this is an ideal site to investigate possible HONO sources and to gain a better
27 understanding of HONO chemistry.

28 **2 Instrumentation**

29 HONO was measured with a commercial Long Path Absorption Photometry instrument (effective light path 1.5 m,
30 LOPAP, Quma, Wuppertal, Germany). LOPAP has a collecting efficiency of >99% for HONO and a detection limit
31 of 4 pptv at a time resolution of 30s. To avoid potential interferences induced by long inlet lines and heterogeneous
32 formation or loss of HONO on the inlet walls, respectively (Kleffmann et al., 1998; Zhou et al., 2002b; Su et al.,
33 2008b), HONO was collected by a sampling unit installed directly in the outdoor atmosphere, i.e., placed on a mast
34 at a height of 5.8 meters above ground installed at the edge of a laboratory container. Furthermore, the LOPAP has
35 two stripping coils placed in series to reduce known interfering signals (Heland et al., 2001). In the first stripping coil
36 HONO is quantitatively collected. Due to the acidic stripping solution interfering species are collected less

1 efficiently but in both channels. The true concentration of HONO is obtained by subtracting the inferences quantified
2 in the second channel (in this study average 1 pptv, at most 5 pptv) from the total signal obtained from the first
3 channel. For a more detailed description of LOPAP, see Heland et al. (2001). This correction of chemical
4 interferences ascertained excellent agreement with the (absolute) DOAS measurements, both in a smog chamber and
5 under urban atmospheric conditions (Kieffmann et al., 2006). A possible interference from peroxyacetic acid (HNO_4)
6 has been proposed (Liao et al., 2006; Kerbrat et al., 2012; Legrand et al., 2014), but this will be insignificant at the
7 high temperatures during CYPHEX, at which HNO_4 is unstable. The stripping coils are temperature controlled by a
8 water-based thermostat and the whole external sampling unit is shielded from sunlight by a small plastic housing.
9 The reagents were all high purity grade chemicals, i.e., hydrochloric acid (37%, for analysis; Merck), sulfanilamide
10 (for analysis, >99%; AppliChem) and N-(1-naphthyl)-ethylenediamine dihydrochloride (for analysis, >98%;
11 AppliChem). For calibration Titrisol® 1000 mg NO_2^- (NaNO_2 in H_2O ; Merck) was diluted to 0.0015 and 0.005 mg/L
12 NO_2^- . For preparation all solutions and for cleaning of the absorption tubes 18 M Ω H_2O was used. [-The accuracy of
13 the HONO measurements was 10%, based on the uncertainties of liquid and gas flow, concentration of calibration
14 standard and regression of calibration.](#)

15 NO and NO_2 measurements were made with a modified commercial chemiluminescence Detector (CLD 790 SR)
16 originally manufactured by ECO Physics (Duernten, Switzerland). The two-channel CLD based on the
17 chemiluminescence of the reaction between NO and O_3 was used for measurements of NO and NO_2 . NO_2 was
18 measured as NO using a photolytic converter from Droplet Measurement Technologies, Boulder USA. In current
19 study, data were obtained at a time resolution of 5 seconds. The CLD detection limits (determined by continuously
20 measuring zero air at measuring site) for NO and NO_2 measurements were 5 pptv and 20 pptv, respectively for an
21 integration period of 5 s. O_3 was measured with a standard UV photometric detector (Model 49, Thermo
22 Environmental Instruments Inc.) with a detection limit of 1 ppb. Data are reported for an integration period of 60 s.
23 The total uncertainties (2σ) for the measurements of NO, NO_2 and O_3 were determined to be 20%, 30% and 5%,
24 respectively, based on the reproducibility of in-field background measurements, calibrations, the uncertainties of the
25 standards and the conversion efficiency of the photolytic converter (Li et al., 2015).

26 OH and HO_2 radicals were measured using the HydrOxyl Radical measurement Unit based on fluorescence
27 Spectroscopy (HORUS) setup developed at the Max Planck Institute for Chemistry (Mainz, Germany). HORUS is
28 based on laser induced fluorescence- fluorescence assay by gas expansion (LIF-FAGE) technique, wherein OH
29 radicals are selectively excited at low pressure by pulsed UV light at around 308 nm, and the resulting fluorescence
30 of OH is detected using gated microchannel plate (MCP) detectors (Martinez et al., 2010; Hens et al., 2014). [The
31 HORUS instrument had an inlet pre-injector \(IPI\) \(Novelli et al. 2014\) which allows the periodic addition of propane
32 to scavenge the atmospheric OH radicals. This procedure allows the removal of potential interference species.](#) HO_2 is
33 estimated by converting atmospheric HO_2 into OH using NO, and detecting the additional OH formed. The
34 instrument is calibrated by measuring signals from known amounts of OH and HO_2 generated by photolysis of water
35 vapor in humidified zero air. [The accuracy \(2 sigma\) of the OH measurements was 29% and the precision \(1 sigma\)
36 was \$4.8 \times 10^5\$ molecules \$\text{cm}^{-3}\$.](#)

37

1 Photolysis frequencies were determined using a spectroradiometer (Metcon GmbH) with a single monochromator
2 and 512 pixel CCD-array as detector (275-640 nm). The thermostatted monochromator/detector unit was attached via
3 a 10 m optical fiber to a 2-II integrating hemispheric quartz dome. The spectroradiometer was calibrated prior to the
4 campaign using a 1000 W NIST traceable irradiance standard. J-values were calculated using molecular parameters
5 recommended by the IUPAC and NASA evaluation panels (Sander et al., 2011; IUPAC, 2015). The J-value for
6 HONO was not corrected for upwelling UV radiation and is estimated to have an uncertainty of ~10 % (Bohn et al.,
7 2008).

8 Aerosol measurements were also performed during the campaign. In this study particulate nitrate and aerosol surface
9 data were used. These were detected by high resolution – time of flight – aerosol mass spectrometer (HR-ToF-AMS,
10 Aerodyne Research Inc., Billerica, MA USA) and scanning mobility particle sizer (SMPS 3936, TSI, Shoreview,
11 MN USA) and aerodynamic particle sizer (APS 3321, TSI), respectively. The mobility and aerodynamic based size
12 distributions were combined based on the algorithm proposed by Khlystov et al. (2004).

13 The volatile organic compounds (VOC) including α -pinene, β -pinene, isoprene, Δ^3 -carene, limonene and DMS
14 (dimethyl sulfide) were detected by a commercial Gas Chromatography-Mass Spectrometry (GC-MS) system (MSD
15 5973; Agilent Technologies GmbH) coupled with an air sampler and a thermal desorber unit (Markes International
16 GmbH). The VOCs were trapped at 30°C on a low-dead-volume quartz cold trap (U-T15ATA; Markes International
17 GmbH) filled with two bed sorbent (Tenax TA and Carbograph I). The cold trap was heated to 320°C and the sample
18 was transferred to a 30m GC column (DB-624, 0.25mm I.D., 1.4 μ m film; J&W Scientific). The temperature of the
19 GC oven was programmed to be stable at 40°C for 5mins and then rising with a rate of 5°C/min up to 140°C.
20 Following, the rate was increased to 40°C/min up to 230°C where it was stabilized for 3min. Each sample was taken
21 every 45mins and calibrations, using a commercial gas standard mixture (National Physical Laboratory, UK), were
22 performed every 8-12 samples.

23 ~~Formaldehyde (HCHO) was measured with a commercial analyzer based on the Hantzsch reaction. The product of
24 the reaction of HCHO with acetyl acetone and ammonia absorbs light at 410 nm and fluoresces at 510 nm which is
25 detected (AL4011, Aerolaser GmbH, Garmisch-Partenkirchen, Germany).~~

26 Carbon monoxide was measured by infrared absorption spectroscopy using a room temperature quantum cascade
27 laser at a time resolution of 1 s. Data are reported as 60 s averages with a total uncertainty of ~10% mainly
28 determined by the uncertainty of the used NIST standard (Li et al., 2015).

29 Meteorological parameters (temperature, relative humidity, wind speed and wind direction, pressure, solar radiation,
30 precipitation) were detected by the weather station Vantage Pro2 from DAVIS.

31 Besides GC-MS all other operating instruments had time resolutions between 20 s and 5 min. For most analyses in
32 this study the data were averaged to 10 min. When GC-MS data were included in the evaluation 1 hour averaged data
33 were used.

34 3 Site description

35 Cyprus is a 9251 km² island in the South-East Mediterranean Sea (fig. 1). The measuring site was located on a
36 military compound in Ineia, Cyprus (N 34.9638, E 32.3778), about 600 m above sea level and approximately 5.5 - 8

1 km from the coast line (in the main wind direction W-SW). The field site is characterized by light vegetation cover, mainly comprising small shrubs like *Pistacia lentiscus*, *Sacopoterium spinosum*, and *Nerium oleander*, herbs like *Inula viscosa* and *Foeniculum vulgare* and few typical Mediterranean trees like *Olea europaea*, *Pinus* sp., and *Ceratonia siliqua*. The area within a radius of about 15 km around the station is only weakly populated. Paphos (88,266 citizens) is located 20 km south of the field site, Limassol (235,000), Nicosia (325,756) and Larnaca (143,367) are 70, 90 and 110 km in the E-SE, respectively (population data according to statistical service of the republic of Cyprus, www.cystat.gov.cy, census of population Oct 2011). During the campaign (07.07. - 04.08.2014), clear sky conditions prevailed and occasionally clouds skimmed the site. No rain was observed, but the elevated field site was impacted by fog during nighttime and early morning due to adiabatic cooling of ascending marine humid air masses. Temperature ranged from 18 to 28°C. Within the main local wind direction of SW (fig. 2A) there was no direct anthropogenic influence resulting in clean humid air from the sea. Analysis of 48-hours back trajectories showed mainly two source regions of air mass origin (fig. 2B). Approximately half (46%) of the campaign the air masses came from the West of Cyprus spending most of their time over the Mediterranean Sea prior to arriving at the site. During the remaining half of the campaign air masses originated from the North of Cyprus, from East European countries (Turkey, Bulgaria, Rumania, Ukraine and Russia). Westerly air masses have been shown to exhibit lower concentration of gaseous and aerosol pollutants than the predominant northerly air masses that typically reach the site (Kleanthous et al., 2014). They spent more time over continental terrestrial surface and were likely to be additionally affected by biomass burning events detected in East Europe within the measurement periods (FIRMS, MODIS, web fire mapper, fig. S1). Previous back trajectory studies in the eastern Mediterranean support this assumption (Kleanthous et al., 2014; Pikridas et al., 2010). Most of the time the advected air mass was loaded with high humidity as a result of sea breeze circulation. Two periods of about 4 days with lower relative humidity occurred. These two situations will be contrasted below.

23 4 Results

24 The concentrations of HONO and other atmospheric trace gases as well as meteorological conditions observed on
25 Cyprus from 7th July 2014 to 3rd August 2014 are shown in fig. 3. In general, low trace gas mixing ratios were
26 indicative of clean marine atmospheric boundary conditions, as pollutants are oxidized by OH during the relatively
27 long air transport time over the Mediterranean sea (more than 30 h), and without significant impact of direct
28 anthropogenic emissions.

29 Ambient HONO mixing ratios ranged from below detection limit (< 4 pptv) to above 300 pptv. Daily average HONO
30 was 35 pptv (\pm 25 pptv; 1 σ standard deviation, following alike). The daily average NO₂ and NO mixing ratios were
31 140 \pm 115 and 20 \pm 35 pptv respectively, but showed intermittent peaks up to 50 ppbv when sampling air was
32 streamed from the diesel generator used to power the station, from the access route or the parking lot by local winds
33 (easterly, fig S2). These incidents, which account for 4% of the campaign time, were classified as local air pollution
34 events and were omitted from analysis. Mean O₃ and CO mixing ratios were 72 \pm 12 ppb and 98 \pm 11 ppbv
35 respectively. OH radicals ranged from below detection limit (1x10⁵ molecules cm⁻³) during nighttime to 8x10⁶
36 molecules cm⁻³ during daytime (see fig. S3). Daytime HO₂/OH ratio ranged from 100 to 150. The mixing ratios of

1 NO₂, O₃ and CO varied in unison, and were significantly ($p < 0.05$) higher during periods when air masses originated
2 from East Europe (brownish bar in fig. 3a lower panel), indicative of air pollution and shorter transport times
3 compared to western Europe (NO₂: Northerly: 144 ± 130 pptv, westerly: 127 ± 106 pptv; O₃: Northerly: 74 ± 11
4 ppbv, westerly: 66 ± 12 ppbv; CO: Northerly: 101 ± 9 ppbv, westerly: 90 ± 10 ppbv). In contrast, NO and HONO
5 mixing ratios were slightly higher when air masses came from Western Europe and over the sea (NO: Northerly: 17
6 ± 35 pptv, westerly: 20 ± 44 pptv; HONO: Northerly: 32 ± 26 pptv, westerly: 38 ± 22 pptv).

7 Besides two different air mass origins, two periods with different behaviour of relative humidity were identified
8 illustrated by blue and yellow boxes in fig. 3(a and b). In both periods we found northerly and westerly air mass
9 origins. The diel profiles of trace gas mixing ratios and meteorological variables of the humid period (blue box) are
10 shown in Fig. 4a, the ones of the dry period (yellow box) in Fig 4b. During the drier period HONO concentrations
11 are stable and low (6 pptv) during night, while mean nighttime HONO mixing ratios during the humid period (fig.
12 4a) showed an expected slow increase of about 20 pptv (from 20 to 40 pptv), as anticipated from heterogeneous
13 production and accumulation within a nocturnal boundary layer characterized by a stable stratification and low wind
14 speed (Acker et al., 2005; Su et al., 2008b; Li et al., 2012). During both periods, but more pronounced in the drier
15 period, HONO rapidly increased by a factor of 2 within two hours after sunrise and then slowly decreased until
16 sunset. Similar profiles were also observed for other trace gases like isoprene or DMS which are transported in
17 upslope winds. Strong HONO morning peaks and high daytime mixing ratios suggest a strong daytime source,
18 compensating the short atmospheric lifetime (15 min) caused by fast photolysis.

19 Mean NO mixing ratios were close to the detection limit (52 pptv) during night and increased after sunrise (06:00
20 local time LT) to mean values of 60 pptv (peak 150 pptv) at 09:00 LT, prior to declining for the rest of the day until
21 sunset (20:00 LT). In the absence of local NO sources low nighttime values are a result of the conversion of NO to
22 NO₂ by O₃ which was continuously high (Hosaynali-Beygi et al., 2011). The diel profiles of NO mixing ratios
23 followed closely those of HONO mixing ratios. This similarity and their dependency on relative humidity are
24 suggestive of a common source for both reactive nitrogen species.

25 NO₂ mixing ratios were somewhat lower during nighttime, but in general the diel variability remained in a narrow
26 range between 100 and 200 pptv. Likewise, the diel courses of O₃ and CO mixing ratios revealed relatively low
27 day/night variability in a range of 65-75 and 90-100 ppb, respectively.

28 5 Discussion

29 Low NO_x conditions at this remote field site in photochemically aged marine air were found to be an ideal
30 prerequisite to trace yet un-defined local HONO sources. On Cyprus, diel profiles of HONO showed peak values in
31 the late morning and persistently high mixing ratios during daytime, as has been reported for some other remote
32 regions (Acker et al., 2006a; Zhou et al., 2007; Huang et al., 2002). This is not the case for rural and urban sites,
33 where atmospheric HONO mixing ratios are normally observed to continuously build up during nighttime
34 presumably due to heterogeneous reactions involving NO_x and decline in the morning due to strong
35 photodissociation (e.g., Elshorbany et al., 2012 and references therein).

1 The diel HONO/NO_x ratio (fig. 4a+b, third panel) shows consistently high values during the humid period (fig. 4a)
 2 and significant diel variation for the dry case (fig. 4b) with higher values during day. The ratio (average 0.33 and
 3 peak values greater than 2) is higher than that reported for most other regions, suggesting a strong impact of local
 4 HONO sources. Elshorbany et al. (2012) investigated data from 15 different urban and rural field measurement
 5 campaigns around the globe, and came up with a robust representative mean atmospheric HONO/NO_x ratio as low
 6 as 0.02. However, high values were observed at remote mountain sites, with mean values of 0.23 (up to ≈0.5 in the
 7 late morning; Zhou et al., 2007) or 0.2–0.4 at remote arctic/polar sites (Li, 1994; Zhou et al., 2001; Beine et al.,
 8 2001; Jacobi et al., 2004; Amoroso et al., 2010). Legrand et al. (2014) observed HONO/NO_x ratios between 0.27 and
 9 0.93 during experiments with irradiated Antarctic snow depending on radiation wavelength, temperature and nitrate
 10 content. Elevated HONO/NO_x ratios at low NO_x levels show the importance of HONO formation mechanisms other
 11 than heterogeneous NO_x reactions.

12 5.1 Nighttime HONO accumulation

13 Between 18:30 – 7:30 LT HONO has an atmospheric lifetime of more than 45 min and [OH] is low, just about 1x10⁵
 14 molecules cm⁻³, so that the calculation of HONO at photostationary state [HONO]_{pss} (R1-R3) at night is not
 15 appropriate. Instead, nighttime HONO concentrations can be estimated due to heterogeneous reaction of NO₂
 16 described in Eq. (1) (Alicke et al., 2002+2003; Su et al., 2008b; Soergel et al., 2011b). Three studies in different
 17 environments from a rural forest region in East Germany (Soergel et al., 2011b) and a non-urban site in the Pearl
 18 River delta, China (Su et al., 2008b) to an urban, polluted site in Beijing (Spataro et al., 2013) found a conversion
 19 rate of about 1.6% h⁻¹ (1.1-1.8 % h⁻¹).

$$20 \quad [\text{HONO}]_{\text{het}} = [\text{HONO}]_{\text{evening}} + 0.016 \text{ h}^{-1} [\text{NO}_2] \Delta t, \quad (\text{Eq. 1})$$

21 [HONO]_{het} denotes the accumulation of HONO by heterogeneous conversion of NO₂, [HONO]_{evening} the measured
 22 HONO ~~mixing ratio~~ concentration at 18:30 LT, [NO₂] the measured average NO₂ ~~mixing ratio~~ concentration
 23 between 18:30 and 7:30 LT, Δt time span in hours.

24 Measured and calculated HONO mixing ratios are compared in figure 4 (upper panel). During the humid period,
 25 during night the estimated (according Eq. (1), fig. 4a upper panel, grey line) and observed HONO mixing ratios are
 26 in good agreement (R² = 0.9). During the drier period the observed HONO mixing ratios were lower than the ones
 27 calculated with a NO₂ conversion rate of 1.6% h⁻¹. ~~But Kleffmann et al., 2003 found a smaller conversion rate of 6 ×~~
 28 ~~10⁻⁷ s⁻¹ (0.22% h⁻¹) for rural forested land in Germany which matches better to the observed nighttime HONO~~
 29 ~~concentration during drier period (fig. 4b upper panel, dark grey line). Here the approach for the nighttime~~
 30 ~~conversion frequency by e.g. Alicke et al., 2002+2003, Su et al., 2008b or Soergel et al., 2011b (rate =~~
 31 ~~$\frac{\text{HONO}_{t2} - \text{HONO}_{t1}}{\Delta t \cdot \text{NO}_2}$) was used. The 7 days average conversion rate for the dry nights was 0.36% h⁻¹ (fig. 4b, upper panel,~~
 32 ~~black line), comparable to results of Kleffmann et al. (2003) reporting a conversion rate of 6 × 10⁻⁷ s⁻¹ (0.22% h⁻¹) for~~
 33 ~~rural forested land in Germany.~~

34 As already mentioned above, it is apparent that under low RH conditions during night, HONO mixing ratios were
 35 much lower than under humid conditions, and HONO morning peaks were most pronounced (compare Fig. 4a and
 36 4b: humid/dry). Both HONO (Donaldson et al., 2014a) and NO₂ (Wang et al., 2012; Liu et al., 2015) uptake

1 coefficients have recently been reported to be much stronger for dry soil, or at low RH, respectively, which is in line
2 with HONO on Cyprus being close to the detection limit in nights with low relative humidity. On the other hand, it
3 has been shown on glass and on soil proxies that the yield of HONO formation from NO₂ on surfaces is low under
4 dry conditions, but sharply increases at RH >30% (Liu et al., 2015) or >60% (Finlayson-Pitts et al., 2003). On
5 Cyprus the strong morning HONO peaks after dry nights were accompanied by an increase in relative humidity from
6 40 to 80%. Deposited and accumulated NO₂ on dry soil surfaces could be released as HONO at high rates under
7 elevated RH conditions. In contrast, in a humid regime HONO mixing ratios were continuously high during
8 nighttime and showed less pronounced morning peaks, suggesting lower nighttime deposition of NO₂ and lower
9 HONO emissions in the morning, respectively.

10 As morning HONO peak mixing ratios were most pronounced after dry nights on Cyprus, our observations are to
11 some extent contradictory to earlier results that have proposed that dew formation on the ground surface may be
12 responsible for HONO nighttime accumulation in the aqueous phase, followed by release from this reservoir after
13 dew evaporation the next morning (Zhou et al., 2002a, Rubio et al., 2002, He et al., 2006). We cannot rule out that
14 the latter could have contributed to nighttime accumulation of HONO during humid conditions, as we had no means
15 to measure dew formation at the site, and high daytime HONO mixing ratios were observed under all humidity
16 regimes. However, kinetic models of competitive adsorption of trace gases and water onto particle surfaces predict
17 exchange behavior explicitly distinct from the liquid phase (Donaldson et al., 2014a). The nitrogen composition in
18 thin water films (few water molecular monolayers) is complex, including HONO, NO, HNO₃, water–nitric acid
19 complexes, NO₂⁺ and N₂O₄ (Finlayson-Pitts et al., 2003). With only small amounts of surface-bound water, nitric
20 acid is largely undissociated HNO₃ and is assumed to be stabilized upon formation of the HNO₃–H₂O complexes
21 (hydrates), which have unique reactivity compared to nitric acid water aqueous solutions, where it is dissociated H⁺
22 and NO₃⁻ ions (Finlayson-Pitts et al., 2003). Likewise, HONO formation rates in surface bound water are about four
23 orders of magnitude larger than expected for the aqueous phase reaction (Pitts et al., 1984).

24 Diel HONO profiles very similar to those on Cyprus with a late morning maximum and late afternoon/early evening
25 minimum have been observed at the Meteorological Observatory Hohenpeissenberg, a mountain-top site in Germany
26 (Acker et al., 2006a) and by Zhou et al. (2007) at the summit of Whiteface Mountain in New York State. For the
27 latter study, formation of dew could be ruled out as relative humidity was mostly well below saturation. Zhou et al.
28 (2007) argued that the high HONO mixing ratios during morning and late morning can be explained by mountain up-
29 slope flow of polluted air from the cities at the foot of the mountain that results from ground surface heating. On
30 Cyprus the sea breeze, driven by the growing difference between sea and soil surface temperature, brings air to the
31 site which interacted with the soil surface and vegetation and is loaded by respective trace gas emissions. This is
32 endorsed by the simultaneous increase of DMS and isoprene, markers for transportation of marine air and emission
33 by vegetation. In the late afternoon, when the surface cools, down-welling air from aloft would dominate, being less
34 influenced by ground surface processes. Zhou et al. (2007) could show that noontime HONO mixing ratios and
35 average NO_y during the previous 24-hour period were strongly correlated, much better than instantaneous
36 HONO/NO_y or HONO/NO_x, which is in line with N-accumulation on soil surfaces as discussed above.

5.2 Daytime HONO budget

During daytime (7:30 to 18:00 LT, with HONO lifetime being between 10 and less than 30 min), $[\text{HONO}]_{\text{PSS}}$, the photostationary HONO concentration resulting from gas phase chemistry can be calculated according to Eq. (2) (Kleffmann et al., 2005):

$$[\text{HONO}]_{\text{PSS}} = \frac{k_1[\text{OH}][\text{NO}]}{k_2[\text{OH}] + J_{\text{HONO}}} \quad (\text{Eq.2})$$

where k_1 and k_2 are the temperature dependent rate constants for the gas phase HONO formation from NO and OH and the loss of HONO by reaction of HONO and OH, respectively (Atkinson et al., 2004; e.g. at 23.0°C a typical temperature during this study $k_1 \approx 1.36 \times 10^{-11} \text{ cm}^3 \text{ s}^{-1}$; $k_2 \approx 6.01 \times 10^{-12} \text{ cm}^3 \text{ s}^{-1}$). J_{HONO} is the photolysis frequency of HONO, which was measured with a spectroradiometer. $[\text{NO}]$ is the observed NO concentration. Since OH data were available only on a few days, diel variations of $[\text{OH}]$ were averaged (see fig. S3).

As has been previously established by many other studies (Su et al., 2008a; Michoud et al., 2014; Soergel et al., 2011a), homogeneous gas-phase chemistry alone fails to reflect observed HONO mixing ratios. Observed daytime values were up to 30 times higher than calculated based on PSS, indicating strong additional local daytime sources of HONO. Lee et al. (2013) argue that the HONO PSS assumption might overestimate the strength of any un-identified source, if the transport time from nearby NO_x emission sources to the measurement site is less than the time required for HONO to reach PSS. In this study, the missing source was calculated according to Su et al., 2008a (eq.3), where PSS was not assumed. Also in our measurements, $d\text{HONO}/dt$ was not equal to zero, as HONO was not at PSS.

$$S_{\text{HONO}} = J_{\text{HONO}}[\text{HONO}] + k_2[\text{OH}][\text{HONO}] - k_1[\text{OH}][\text{NO}] - k_{\text{het}}[\text{NO}_2] + \frac{\Delta[\text{HONO}]}{\Delta t} \quad (\text{Eq.3})$$

with $[\text{HONO}]$ being the measured HONO concentration and k_{het} the heterogeneous conversion rate of NO₂ to HONO, which was discussed above to be 1.6% h⁻¹ during the wet period and 0.36% h⁻¹ during the dry period. $\Delta[\text{HONO}]/\Delta t$ is the observed change of HONO concentration unequal to 0. The uncertainty of the calculated missing source S_{HONO} was estimated to be about 16% based on the Gaussian error propagation of instrument uncertainties of HONO, NO, NO₂, J and OH.

Nevertheless, at the study site of Cyprus, the mean upwind distance between the measurement site and the coast line was about 6 km, and the mean wind velocity was about 3 m s⁻¹. Accordingly, the respective air mass travel time over land is estimated to be about half an hour, which is somewhat longer than the daytime lifetime of HONO and might provide enough time for the equilibrium processes. Furthermore and in a strong contrast to Lee et al. (2013), at the Cyprus site the concentrations of HONO precursors (NO and OH) were extremely low, by far too low to explain the observed HONO concentrations. The strength of these sources (S_{HONO}) can be calculated by following equation:

$$S_{\text{HONO}} = ([\text{HONO}]_{\text{measured}} - [\text{HONO}]_{\text{PSS}}) \cdot (k_2[\text{OH}] + J_{\text{HONO}}) \quad (\text{Eq. 3})$$

In the late morning (around 10:00 LT) the unknown source was at its maximum with peak production rates of up to $3.4 \times 10^6 \text{ molecules cm}^{-3} \text{ s}^{-1}$, and a daytime average of about $1.3 \times 10^6 \text{ cm}^{-3} \text{ s}^{-1}$, which is in good agreement with other studies at rural sites like a mountain site at Hohenpeissenberg ($(3 \pm 1) \times 10^6 \text{ cm}^{-3} \text{ s}^{-1}$, at $\text{NO}_x \approx 2 \text{ ppbv}$, Acker et al., 2006a), a deciduous forest site in Jülich ($3.45 \times 10^6 \text{ molecules cm}^{-3} \text{ s}^{-1}$, at $\text{NO} \approx 250 \text{ pptv}$, Kleffmann et al., 2005) and a pine forest site in South-West Spain $0.74 \times 10^6 \text{ molecules cm}^{-3} \text{ s}^{-1}$, at $\text{NO}_x \approx 1.5 \text{ ppbv}$, Soergel et al., 2011a) but

1 smaller than at urban sites in Houston ($4\text{-}6 \times 10^6 \text{ cm}^{-3} \text{ s}^{-1}$, at $\text{NO}_x \approx 6 \text{ ppbv}$, Wong et al., 2012), Beijing ($7 \times 10^6 \text{ cm}^{-3} \text{ s}^{-1}$,
2 at $\text{NO}_x \approx 15 \text{ ppbv}$, Yang et al., 2014) and South China ($5.25 \pm 3.75 \times 10^6 \text{ cm}^{-3} \text{ s}^{-1}$, at $\text{NO}_x \approx 20 \text{ ppbv}$, Li et al., 2012; or
3 $1\text{-}4 \times 10^7 \text{ cm}^{-3} \text{ s}^{-1}$, at $\text{NO}_x \approx 35 \text{ ppbv}$, Su et al., 2008a).

4 The contributions of gas phase reactions and the heterogeneous reaction of NO_2 (conversion rate (a) $1.6\% \text{ h}^{-1}$ and (b)
5 $0.36\% \text{ h}^{-1}$) to the HONO budget are illustrated in fig. 5, exemplary. For both periods the contributions are quiet
6 similar just the absolute values are different. To compensate the strong loss via photolysis a comparable strong
7 unknown source is necessary as the heterogeneous NO_2 conversion or the gasphase reaction of OH and NO are
8 insignificant.

9 In polluted regions with moderate to high NO_x concentrations, HONO sources have often been linked with $[\text{NO}_2]$ or
10 $[\text{NO}_x]$ (Acker et al., 2005, Li et al., 2012, Levy et al., 2014, Soc̈erger et al., 2011a, Wentzel et al., 2010). Under the
11 prevailing low NO_x conditions during CYPHEX ($< 250 \text{ pptv}$), correlation analysis (see table 1) of S_{HONO} with $[\text{NO}_2]$
12 ($R^2 = 0.4450$) and $[\text{NO}_2] \cdot \text{RH}$ ($R^2 = 0.4651$) indicate no significant impact of instantaneous heterogeneous formation
13 of HONO from NO_2 . Better correlations of S_{HONO} with J_{NO_2} ($R^2 = 0.674$) and $J_{\text{NO}_2} \cdot [\text{NO}_2]$ ($R^2 = 0.842$) indicate a
14 photo-induced conversion of NO_2 to HONO as already suggested by George et al. (2005) or Stemmler et al. (2006,
15 2007). Lee et al. (2016) found even lower correlation with $[\text{NO}_2]$ ($R^2 = 0.0001$) but similar good correlation with
16 $J_{\text{NO}_2} \cdot [\text{NO}_2]$ ($R^2 = 0.70$) at an urban background site in London. Other light dependent reactions such as the photolysis
17 of nitrate might additionally contribute to high daytime HONO. It is unlikely that aerosol surfaces played an
18 important role in heterogeneous conversion of NO_2 as the mean observed aerosol surface concentration was only
19 about $300 \mu\text{m}^2 \text{ cm}^{-3}$. Based on a formula for photo enhanced conversion of NO_2 on humic acid aerosols which was
20 derived by Stemmler et al. (2007) a HONO formation rate of only $5.1 \times 10^2 \text{ molecules cm}^{-3} \text{ s}^{-1}$ can be estimated.
21 Likewise, Soc̈erger et al. (2015) showed that HONO fluxes from light-activated reactions of NO_2 on humic acid
22 surfaces at low NO_2 levels ($< 1 \text{ ppb}$ and thus comparable to concentrations observed in this study) saturated at
23 around $0.0125 \text{ nmol m}^{-2} \text{ s}^{-1}$. Therefore heterogeneous aerosol surface reactions can be neglected as HONO sources at
24 the prevailing low NO_x levels.

25 Likewise, the nitrate concentrations of highly acidic marine aerosols particulate matter as measured by HR-ToF-
26 AMS (PM1 fraction, mean $0.075 \mu\text{g m}^{-3}$) were too low to account for significant photolytic HONO production
27 ($1.7 \times 10^2 \text{ molecules cm}^{-3} \text{ s}^{-1}$ or 0.01% of S_{HONO}) calculated by Eq. (4):

$$28 \quad S_{\text{photo_NO}_3^-} = [\overline{\text{NO}_3^-}] \cdot J_{\text{NO}_3^-} \quad (\text{Eq. 4})$$

29 with $S_{\text{photo_NO}_3^-}$ the source strength of HONO by photolysis of nitrate, $[\overline{\text{NO}_3^-}]$ the mean particulate nitrate
30 concentration and $J_{\text{NO}_3^-}$ the photolysis frequency of nitrate (aqueous) at noon ($3 \times 10^{-7} \text{ s}^{-1}$, Jankowski et al., 1999).

31 Recently an enhancement of the photolysis frequency of particulate nitrate relative to gaseous or aqueous nitrate was
32 found (Ye et al., 2016). But even with this enhanced rate of $2 \times 10^{-4} \text{ s}^{-1}$ not more than $1.1 \times 10^5 \text{ molecules cm}^{-3} \text{ s}^{-1}$ (8%
33 of S_{HONO}) HONO would be produced.

5.3 Common daytime source of HONO and NO

During CYPHEX, good correlation was found between [HONO] or S_{HONO} and [NO] ($R^2 = 0.86$ and 0.640 , respectively), indicating that both may have a common source. A missing source of NO ~~based on the photostationary state~~ can be calculated as shown in Eq. (5) ~~and (6)~~.

$$[\text{NO}]_{\text{PSS}} = \frac{J_{\text{NO}_2}[\text{NO}_2] + J_{\text{HONO}}[\text{HONO}]}{k_1[\text{OH}] + k_3[\text{HO}_2] + k_4[\text{O}_3] + k_5[\text{RO}_2]} \quad (\text{Eq. 5})$$

$$S_{\text{NO}} = \left([\text{NO}]_{\text{measured}} - [\text{NO}]_{\text{PSS}} \right) \cdot (k_1[\text{OH}] + k_3[\text{HO}_2] + k_4[\text{O}_3] + k_5[\text{RO}_2]) + k_1[\text{OH}][\text{NO}] + k_3[\text{HO}_2][\text{NO}] + k_4[\text{O}_3][\text{NO}] + k_5[\text{RO}_2][\text{NO}] - J_{\text{NO}_2}[\text{NO}_2] - J_{\text{HONO}}[\text{HONO}] + \frac{\Delta[\text{NO}]}{\Delta t} \quad (\text{Eq. 5b})$$

k_3 and k_4 are the temperature dependent rate constants for the reaction of NO with HO_2 and O_3 , respectively (Atkinson et al., 2004; at 23°C : $k_3 \approx 8.96 \times 10^{-12} \text{ cm}^3 \text{ s}^{-1}$; $k_4 \approx 1.68 \times 10^{-14} \text{ cm}^3 \text{ s}^{-1}$), k_5 is the rate constant for the reaction of NO and organic peroxy radicals which was assumed to be the same as for the reaction $\text{NO} + \text{CH}_3\text{O}_2$ ($7.7 \times 10^{-12} \text{ cm}^3 \text{ s}^{-1}$ at 298K , Ren et al., 2010; Sander et al., 2011). Like [OH] also [HO₂] was measured only on a few days and therefore mean diel data were used (fig. S3). Total [RO₂] was estimated to be maximum $1.6 \times [\text{HO}_2]$ (Ren et al., 2010; Hens et al., 2014). Using a RO₂/HO₂ ratio of 1.2 the absolute values of S_{NO} are reduced by 0.3 to 5.5%. The budget analysis for NO for both humidity regimes is illustrated in fig. S4.

For NO_x, an unexpected deviation from the PSS, or Leighton ratio, respectively, of clean marine boundary layer air has been observed previously, invoking a hitherto unknown NO sink, or pathway for NO to NO₂ oxidation, other than reactions with OH, HO₂, O₃ and organic peroxides (Hosaynali-Beygi et al., 2011). On Cyprus, two different atmospheric humidity regimes can be differentiated. Under dry conditions (RH < 70%, yellow boxes in fig. 3) and higher NO_x concentrations (>150 pptv) S_{NO} is negative, implying a net NO sink of up to $6.4 \times 10^7 \text{ molecules cm}^{-3} \text{ s}^{-1}$ resembling the above mentioned PSS deviations in remote marine air masses (see fig. 6 and 7). However, during humid conditions (RH > 70, blue boxes in fig. 3) S_{NO} was positive with values of up to $5.1 \times 10^7 \text{ molecules cm}^{-3} \text{ s}^{-1}$. Due to low and invariant acetonitrile levels, anthropogenic activity and local biomass burning can be excluded as NO source at this specific site. A net NO source during humid conditions is assumed to result from (biogenic) NO emission from soil. -As shown in fig. 8, the PSS-based S_{HONO} and S_{NO} (time of day-averaged, excluding 3 days as there are transition days 25.7. and 2.8. or the RH changed too quickly 15.7.) were highly correlated ($R^2 = 0.728$), indicative of both reactive N-compounds being emitted from the same local source. Both HONO and NO have been reported to be released from soil, with a strong dependency on soil water content (Su et al., 2011; Oswald et al., 2013; Mantimin et al., 2016). The (dry state) soil humidification threshold level for NO emission is reported to be somewhat higher than for HONO (Oswald et al., 2013), which might explain why a net PSS-based NO source was preferentially calculated for higher relative humidity conditions, while for HONO the PSS indicated a daytime source under all humidity regimes prevailing during the campaign was found. Mantimin et al. (2016) investigated HONO and NO emissions of natural desert soil and with grapes or cotton cultivated soils in an oasis in the Taklamakan desert in the Xinjiang region in China. After irrigation they didn't find direct emission, but when the soil had almost dried out (gravimetric soil water content 0.01-0.3) emissions up to $115 \text{ ng N m}^{-2} \text{ s}^{-1}$ were detected. In addition they observed soil-temperature dependent emission of reactive nitrogen. Analyzing microbial surface

1 communities from drylands, Weber et al. (2015) observed highly correlated NO-N and HONO-N emissions with
 2 Spearman rank correlation coefficients ranging between 0.75 and 0.99. In this study, NO- and HONO-emissions
 3 were observed in drying soils with water contents of 20-30% water holding capacity.
 4 Even though we cannot make firm conclusions regarding the exact mechanism of HONO formation, the above
 5 mentioned correlation analysis (and table 1) reveal that the instantaneous heterogeneous NO₂ conversion is not a
 6 significant HONO source. We propose that HONO is emitted from nitrogen compounds being accumulated on
 7 mountain slope soil surfaces produced either biologically by soil microbiota or from previously deposited NO_y. This
 8 forms the major daytime HONO source responsible for morning concentration peaks and consistently high daytime
 9 mixing ratios at the Cyprus field site. While biological formation is assumed to be more relevant for humid
 10 conditions, physical NO_y accumulation can be assumed to be stronger under dry conditions, as uptake coefficients
 11 for a variety of trace gases were shown to be significantly higher for dry surfaces, among them NO₂ (Wang et al.,
 12 2012, Liu et al., 2015), HONO (Donaldson et al. 2014a) and HCHO (Li et al., 2016). The strongest HONO morning
 13 peaks observed after dry nights were accompanied by an increase in relative humidity driven by the sea breeze (fig.
 14 4b), so we consider HONO being released preferentially under favourable humid conditions.

15 5.4 primary OH production

16 Many studies showed high contribution of HONO photolysis to the OH budget (up to 30% on daily average; Alicke
 17 et al., 2002, Ren et al., 2006). Here the primary OH production rates are calculated based on the main OH forming
 18 reactions, which are the photolysis of ozone O₃ and subsequent reaction with water (R6+7), the photolysis of HONO
 19 (R2) and HCHO (R8-11) and the reaction of alkenes with ozone (R128).



27 Reaction rates were taken from Atkinson et al. (2004) and Atkinson (1997). The water pressure over water was
 28 calculated according to Murphy and Koop (2005). Reactions of O(¹D) and HO₂ not forming OH are also considered.
 29 OH formation yields of the reactions of alkenes with O₃ were taken from Paulson et al. (1999). Photolysis rates (J-
 30 values) and concentrations of relevant compounds were as measured on Cyprus. Isoprene, α-pinene, β-pinene, Δ3-
 31 carene and limonene (VOC) were taken into account as the most relevant alkenes.

32 The results of this study are shown in fig. 9. All four production routes show a clear diel profile with higher
 33 production rates during daytime. In the night only the reaction of alkenes with O₃ produced significant amounts of
 34 OH (2x10⁴ molecules cm⁻³ s⁻¹). With sunrise the other sources become more relevant. During day the photolysis of
 35 HONO and HCHO lead to generates about similar daytime OH production rates of about 0.8-1.5x10⁶ molecules OH
 36 cm⁻³ s⁻¹, which is about 10 times higher than the ozonolysis of alkenes at that time. The maximum OH production

1 rate by O₃ photolysis during daytime is about 1.3x10⁷ molecules cm⁻³ s⁻¹. In the morning (6-8 am) and evening hours
2 (7-8 pm) the contribution of HONO photolysis to the ~~total~~primary OH production is in average 370% (see fig. 9b)
3 with peak values of 650%, which is much higher than the contribution of O₃ photolysis at that time. During the rest
4 of the day the contribution of HONO decreases to 12%. ~~The contribution of HCHO is slightly lower.~~ At noon the
5 most dominant OH source is the photolysis of O₃ (more than 80%) while the contribution of the ozonolysis of
6 alkenes is almost negligible (1-2%). A complete and detailed HO_x budget analysis with CYPHEX data will be
7 published soon.

8 **6 Conclusion**

9 Nitrous acid was found in low concentrations on the east Mediterranean Island of Cyprus during summer 2014.
10 Daytime concentrations were much higher than during the night and about 30 times higher than would be expected
11 by budget analysis based on photostationary state. The unknown source was calculated to be about 1.9x10⁶
12 molecules cm⁻³ s⁻¹ around noon. Low NO_x concentrations, high HONO/NO_x ratio and low correlation between
13 HONO and NO₂ indicate a local source which is independent from NO₂. Heterogeneous reactions of NO₂ on aerosols
14 play an insignificant role during daytime. Emission from soil, either caused by photolysis of nitrate or gas-soil
15 partitioning of accumulated nitrite/nitrous acid, is supposed to have a higher impact on the HONO concentration
16 during this campaign. Also the NO budget analysis showed a missing source in the humid period, which correlates
17 well with the unknown source of HONO, indicating a common source. The most likely source of HONO and NO is
18 the emission from soil.
19 Even though the HONO concentration is only in the lower pptv level, it has a high contribution to the primary OH
20 production in the early morning and evening hours.

21 **Acknowledgement**

22 This study was supported by the Max Planck Society (MPG) and the DFG-Research Center / Cluster of Excellence
23 „The Ocean in the Earth System-MARUM”.

24 We thank the Cyprus Institute and the Department of Labor Inspection for the logistical support, as well as the
25 military staff at the Lara Naval Observatory in Ineia for the excellent collaboration.

26 Furthermore ~~I~~we'd like to thank Mathias Söörger, ~~an experienced colleague from MPI-C~~ for his technical support
27 on experimental set-up of atmospheric HONO measurements.

28 **References**

29 Acker, K., Moller, D., Auel, R., Wieprecht, W., and Kalass, D.: Concentrations of nitrous acid, nitric acid, nitrite and
30 nitrate in the gas and aerosol phase at a site in the emission zone during ESCOMPTE 2001 experiment, Atmospheric
31 Research, 74, 507-524, 2005.

1 Acker, K., Moller, D., Wieprecht, W., Meixner, F. X., Bohn, B., Gilge, S., Plass-Dulmer, C., and Berresheim, H.:
2 Strong daytime production of OH from HNO₂ at a rural mountain site, *Geophysical Research Letters*, 33, 2006a.

3 Acker, K., Febo, A., Trick, S., Perrino, C., Bruno, P., Wiesen, P., Moeller, D., Wieprecht, W., Auel, R., Giusto, M.,
4 Geyer, A., Platt, U., and Allegrini, I.: Nitrous acid in the urban area of Rome, *Atmospheric Environment*, 40, 3123-
5 3133, 2006b.

6 Acker, K., Beysens, D., and Moeller, D.: Nitrite in dew, fog, cloud and rain water: An indicator for heterogeneous
7 processes on surfaces, *Atmospheric Research*, 87, 200-212, 2008.

8 Aliche, B., Platt, U., and Stutz, J.: Impact of nitrous acid photolysis on the total hydroxyl radical budget during the
9 Limitation of Oxidant Production/Pianura Padana Produzione di Ozono study in Milan, *Journal of Geophysical*
10 *Research-Atmospheres*, 107, 2002.

11 [Aliche, B., Geyer, A., Hofzumahaus, A., Holland, F., Konrad, S., Patz, H. W., Schafer, J., Stutz, J., Volz-Thomas,](#)
12 [A., and Platt, U.: OH formation by HONO photolysis during the BERLIOZ experiment, *Journal of Geophysical*](#)
13 [Research-Atmospheres](#), 108, 2003.

14 Ammann, M., Kalberer, M., Jost, D. T., Tobler, L., Rossler, E., Piguet, D., Gaggeler, H. W., and Baltensperger, U.:
15 Heterogeneous production of nitrous acid on soot in polluted air masses, *Nature*, 395, 157-160, 1998.

16 Amoroso, A., Domine, F., Esposito, G., Morin, S., Savarino, J., Nardino, M., Montagnoli, M., Bonneville, J. M.,
17 Clement, J. C., Ianniello, A., and Beine, H. J.: Microorganisms in Dry Polar Snow Are Involved in the Exchanges of
18 Reactive Nitrogen Species with the Atmosphere, *Environmental Science & Technology*, 44, 714-719, 2010.

19 Arens, F., Gutzwiller, L., Baltensperger, U., Gaggeler, H. W., and Ammann, M.: Heterogeneous reaction of NO₂ on
20 diesel soot particles, *Environmental Science & Technology*, 35, 2191-2199, 2001.

21 Arey, J., Atkinson, R., and Aschmann, S. M.: Product study of the gas-phase reactions of monoterpenes with the OH
22 radical in the presence of NO_x, *Journal of Geophysical Research: Atmospheres*, 95, 18539-18546, 1990.

23 Atkinson, R.: Gas-Phase Tropospheric Chemistry of Volatile Organic Compounds: 1. Alkanes and Alkenes, *Journal*
24 *of Physical and Chemical Reference Data*, 26, 215-290, 1997.

25 Atkinson, R., Baulch, D. L., Cox, R. A., Crowley, J. N., Hampson, R. F., Hynes, R. G., Jenkin, M. E., Rossi, M. J.,
26 and Troe, J.: Evaluated kinetic and photochemical data for atmospheric chemistry: Volume I - gas phase reactions of
27 O-x, HO_x, NO_x and SO_x species, *Atmospheric Chemistry and Physics*, 4, 1461-1738, 2004.

28 Aubin, D. G., and Abbatt, J. P. D.: Interaction of NO₂ with hydrocarbon soot: Focus on HONO yield, surface
29 modification, and mechanism, *Journal of Physical Chemistry A*, 111, 6263-6273, 2007.

30 Baergen, A. M., and Donaldson, D. J.: Photochemical Renoxification of Nitric Acid on Real Urban Grime,
31 *Environmental Science & Technology*, 47, 815-820, 2013.

32 Beine, H. J., Allegrini, I., Sparapani, R., Ianniello, A., and Valentini, F.: Three years of springtime trace gas and
33 particle measurements at Ny-Alesund, Svalbard, *Atmospheric Environment*, 35, 3645-3658, 2001.

1 Bejan, I., Abd El Aal, Y., Barnes, I., Benter, T., Bohn, B., Wiesen, P., and Kleffmann, J.: The photolysis of ortho-
2 nitrophenols: a new gas phase source of HONO, *Physical Chemistry Chemical Physics*, 8, 2028-2035, 2006.

3 Beygi, Z. H., Fischer, H., Harder, H. D., Martinez, M., Sander, R., Williams, J., Brookes, D. M., Monks, P. S., and
4 Lelieveld, J.: Oxidation photochemistry in the Southern Atlantic boundary layer: unexpected deviations of
5 photochemical steady state, *Atmospheric Chemistry and Physics*, 11, 8497-8513, 2011.

6 Bianchi, M., Feliatra, F., Tréguer, P., Vincendeau, M.-A., and Morvan, J.: Nitrification rates, ammonium and nitrate
7 distribution in upper layers of the water column and in sediments of the Indian sector of the Southern Ocean, *Deep
8 Sea Research Part II: Topical Studies in Oceanography*, 44, 1017-1032, 1997.

9 Bohn, B., Corlett, G. K., Gillmann, M., Sanghavi, S., Stange, G., Tensing, E., Vrekoussis, M., Bloss, W. J., Clapp, L.
10 J., Kortner, M., Dorn, H. P., Monks, P. S., Platt, U., Plass-Dulmer, C., Mihalopoulos, N., Heard, D. E., Clemitshaw,
11 K. C., Meixner, F. X., Prevot, A. S. H., and Schmitt, R.: Photolysis frequency measurement techniques: results of a
12 comparison within the ACCENT project, *Atmospheric Chemistry and Physics*, 8, 5373-5391, 2008.

13 Bröeske, R., Kleffmann, J., and Wiesen, P.: Heterogeneous conversion of NO₂ on secondary organic aerosol
14 surfaces: A possible source of nitrous acid (HONO) in the atmosphere?, *Atmospheric Chemistry and Physics*, 3, 469-
15 474, 2003.

16 Costabile, F., Amoroso, A., and Wang, F.: Sub-micron particle size distributions in a suburban Mediterranean area.
17 Aerosol populations and their possible relationship with HONO mixing ratios, *Atmospheric Environment*, 44, 5258-
18 5268, 2010.

19 Czader, B. H., Rappenglueck, B., Percell, P., Byun, D. W., Ngan, F., and Kim, S.: Modeling nitrous acid and its
20 impact on ozone and hydroxyl radical during the Texas Air Quality Study 2006, *Atmospheric Chemistry and
21 Physics*, 12, 6939-6951, 2012.

22 Donaldson, M. A., Berke, A. E., and Raff, J. D.: Uptake of Gas Phase Nitrous Acid onto Boundary Layer Soil
23 Surfaces, *Environmental Science & Technology*, 48, 375-383, 2014a.

24 Donaldson, M. A., Bish, D. L., and Raff, J. D.: Soil surface acidity plays a determining role in the atmospheric-
25 terrestrial exchange of nitrous acid, *Proceedings of the National Academy of Sciences*, 111, 18472-18477, 2014b.

26 Duplissy, J., Gysel, M., Alfarra, M. R., Dommen, J., Metzger, A., Prevot, A. S. H., Weingartner, E., Laaksonen, A.,
27 Raatikainen, T., Good, N., Turner, S. F., McFiggans, G., and Baltensperger, U.: Cloud forming potential of
28 secondary organic aerosol under near atmospheric conditions, *Geophysical Research Letters*, 35, 2008.

29 Elshorbany, Y. F., Steil, B., Brühl, C., and Lelieveld, J.: Impact of HONO on global atmospheric chemistry
30 calculated with an empirical parameterization in the EMAC model, *Atmospheric Chemistry and Physics*, 12, 9977-
31 10000, 2012.

32 Finlayson-Pitts, B. J., Wingen, L. M., Sumner, A. L., Syomin, D., and Ramazan, K. A.: The heterogeneous
33 hydrolysis of NO₂ in laboratory systems and in outdoor and indoor atmospheres: An integrated mechanism, *Physical
34 Chemistry Chemical Physics*, 5, 223-242, 2003.

1 Foster, J. R., Pribush, R. A., and Carter, B. H.: THE CHEMISTRY OF DEWS AND FROSTS IN INDIANAPOLIS,
2 INDIANA, Atmospheric Environment Part a-General Topics, 24, 2229-2236, 1990.

3 George, C., Streckowski, R. S., Kleffmann, J., Stemmler, K., and Ammann, M.: Photoenhanced uptake of gaseous
4 NO₂ on solid-organic compounds: a photochemical source of HONO?, Faraday Discussions, 130, 195-210, 2005.

5 Han, C., Liu, Y., and He, H.: Role of Organic Carbon in Heterogeneous Reaction of NO₂ with Soot, Environmental
6 science & technology, 47, 3174-3181, 2013.

7 Harrison, R. M., and Kitto, A. M. N.: EVIDENCE FOR A SURFACE SOURCE OF ATMOSPHERIC NITROUS-
8 ACID, Atmospheric Environment, 28, 1089-1094, 1994.

9 He, Y., Zhou, X. L., Hou, J., Gao, H. L., and Bertman, S. B.: Importance of dew in controlling the air-surface
10 exchange of HONO in rural forested environments, Geophysical Research Letters, 33, 2006.

11 Heland, J., Kleffmann, J., Kurtenbach, R., and Wiesen, P.: A new instrument to measure gaseous nitrous acid
12 (HONO) in the atmosphere, Environmental Science & Technology, 35, 3207-3212, 2001.

13 Hens, K., Novelli, A., Martinez, M., Auld, J., Axinte, R., Bohn, B., Fischer, H., Keronen, P., Kubistin, D., Noelscher,
14 A. C., Oswald, R., Paasonen, P., Petaja, T., Regelin, E., Sander, R., Sinha, V., Sipila, M., Taraborrelli, D., Ernest, C.
15 T., Williams, J., Lelieveld, J., and Harder, H.: Observation and modelling of HO_x radicals in a boreal forest,
16 Atmospheric Chemistry and Physics, 14, 8723-8747, 2014.

17 Huang, G., Zhou, X. L., Deng, G. H., Qiao, H. C., and Civerolo, K.: Measurements of atmospheric nitrous acid and
18 nitric acid, Atmospheric Environment, 36, 2225-2235, 2002.

19 IUPAC: Task Group on Atmospheric Chemical Kinetic Data Evaluation, (Ammann, M., Cox, R.A., Crowley, J.N.,
20 Jenkin, M.E., Mellouki, A., Rossi, M. J., Troe, J. and Wallington, T. J.) <http://iupac.pole-ether.fr/index.html>, 2015.

21 Jacobi, H. W., Bales, R. C., Honrath, R. E., Peterson, M. C., Dibb, J. E., Swanson, A. L., and Albert, M. R.: Reactive
22 trace gases measured in the interstitial air of surface snow at Summit, Greenland, Atmospheric Environment, 38,
23 1687-1697, 2004.

24 Jankowski, J. J., Kieber, D. J., and Mopper, K.: Nitrate and nitrite ultraviolet actinometers, Photochemistry and
25 Photobiology, 70, 319-328, 1999.

26 Jiang, Q. Q., and Bakken, L. R.: Comparison of Nitrosospira strains isolated from terrestrial environments, FEMS
27 Microbiology Ecology, 30, 171-186, 1999.

28 Kalberer, M., Ammann, M., Arens, F., Gaggeler, H. W., and Baltensperger, U.: Heterogeneous formation of nitrous
29 acid (HONO) on soot aerosol particles, Journal of Geophysical Research-Atmospheres, 104, 13825-13832, 1999.

30 Kebede, M. A., Scharko, N. K., Appelt, L. E., and Raff, J. D.: Formation of Nitrous Acid during Ammonia
31 Photooxidation on TiO₂ under Atmospherically Relevant Conditions, Journal of Physical Chemistry Letters, 4,
32 2618-2623, 2013.

1 Kerbrat, M., Legrand, M., Preunkert, S., Gallée, H., and Kleffmann, J.: Nitrous acid at Concordia (inland site) and
2 Dumont d'Urville (coastal site), East Antarctica, *Journal of Geophysical Research: Atmospheres*, 117, D08303,
3 2012.

4 Kessler, C., and Platt, U.: Nitrous Acid in Polluted Air Masses — Sources and Formation Pathways, in: *Physico-
5 Chemical Behaviour of Atmospheric Pollutants*, edited by: Versino, B., and Angeletti, G., Springer Netherlands,
6 412-422, 1984.

7 Kinugawa, T., Enami, S., Yabushita, A., Kawasaki, M., Hoffmann, M. R., and Colussi, A. J.: Conversion of gaseous
8 nitrogen dioxide to nitrate and nitrite on aqueous surfactants, *Physical Chemistry Chemical Physics*, 13, 5144-5149,
9 2011.

10 Khlystov, A., Stanier, C., and Pandis, S. N.: An algorithm for combining electrical mobility and aerodynamic size
11 distributions data when measuring ambient aerosol, *Aerosol Science and Technology*, 38, 229-238, 2004.

12 Kleanthous, S., Vrekoussis, M., Mihalopoulos, N., Kalabokas, P., and Lelieveld, J.: On the temporal and spatial
13 variation of ozone in Cyprus, *Science of The Total Environment*, 476-477, 677-687, 2014.

14 Kleffmann, J., Becker, K. H., and Wiesen, P.: Heterogeneous NO₂ conversion processes on acid surfaces: possible
15 atmospheric implications, *Atmospheric Environment*, 32, 2721-2729, 1998.

16 Kleffmann, J., H. Becker, K., Lackhoff, M., and Wiesen, P.: Heterogeneous conversion of NO₂ on carbonaceous
17 surfaces, *Physical Chemistry Chemical Physics*, 1, 5443-5450, 1999.

18 Kleffmann, J., Kurtenbach, R., Lorzer, J., Wiesen, P., Kalthoff, N., Vogel, B., and Vogel, H.: Measured and
19 simulated vertical profiles of nitrous acid - Part I: Field measurements, *Atmospheric Environment*, 37, 2949-2955,
20 2003.

21 Kleffmann, J., Gavriloiiei, T., Hofzumahaus, A., Holland, F., Kopppmann, R., Rupp, L., Schlosser, E., Siese, M., and
22 Wahner, A.: Daytime formation of nitrous acid: A major source of OH radicals in a forest, *Geophysical Research
23 Letters*, 32, 2005.

24 Kleffmann, J., and Wiesen, P.: Heterogeneous conversion of NO₂ and NO on HNO₃ treated soot surfaces:
25 atmospheric implications, *Atmospheric Chemistry and Physics*, 5, 77-83, 2005.

26 Kurtenbach, R., Becker, K. H., Gomes, J. A. G., Kleffmann, J., Lorzer, J. C., Spittler, M., Wiesen, P., Ackermann,
27 R., Geyer, A., and Platt, U.: Investigations of emissions and heterogeneous formation of HONO in a road traffic
28 tunnel, *Atmospheric Environment*, 35, 3385-3394, 2001.

29 Lammel, G., and Cape, J. N.: Nitrous acid and nitrite in the atmosphere, *Chemical Society Reviews*, 25, 361-369,
30 1996.

31 Langridge, J. M., Gustafsson, R. J., Griffiths, P. T., Cox, R. A., Lambert, R. M., and Jones, R. L.: Solar driven
32 nitrous acid formation on building material surfaces containing titanium dioxide: A concern for air quality in urban
33 areas?, *Atmospheric Environment*, 43, 5128-5131, 2009.

1 Lee, B. H., Wood, E. C., Herndon, S. C., Lefer, B. L., Luke, W. T., Brune, W. H., Nelson, D. D., Zahniser, M. S.,
2 and Munger, J. W.: Urban measurements of atmospheric nitrous acid: A caveat on the interpretation of the HONO
3 photostationary state, *J. Geophys. Res.*, vol. 118, 12274–12281, 2013.

4 Lee, J. D., Whalley, L. K., Heard, D. E., Stone, D., Dunmore, R. E., Hamilton, J. F., Young, D. E., Allan, J. D.,
5 Laufs, S., and Kleffmann, J.: Detailed budget analysis of HONO in central London reveals a missing daytime source,
6 *Atmospheric Chemistry and Physics*, 16, 2747-2764, 2016.

7 Legrand, M., Preunkert, S., Frey, M., Bartels-Rausch, T., Kukui, A., King, M. D., Savarino, J., Kerbrat, M., and
8 Jourdain, B.: Large mixing ratios of atmospheric nitrous acid (HONO) at Concordia (East Antarctic Plateau) in
9 summer: a strong source from surface snow?, *Atmospheric Chemistry and Physics*, 14, 9963-9976, 2014.

10 Lelièvre, S., Bedjanian, Y., Laverdet, G., and Le Bras, G.: Heterogeneous Reaction of NO₂ with Hydrocarbon Flame
11 Soot, *The Journal of Physical Chemistry A*, 108, 10807-10817, 2004.

12 Levy, H.: Normal Atmosphere: Large Radical and Formaldehyde Concentrations Predicted, *Science*, 173, 141-143,
13 1971.

14 Levy, M., Zhang, R., Zheng, J., Zhang, A. L., Xu, W., Gomez-Hernandez, M., Wang, Y., and Olaguer, E.:
15 Measurements of nitrous acid (HONO) using ion drift-chemical ionization mass spectrometry during the 2009
16 SHARP field campaign, *Atmospheric Environment*, 94, 231-240, 2014.

17 Li, J., A. Reiffs, U. Parchatka, and H. Fischer, In situ measurements of atmospheric CO and its correlation with NO_x
18 and O₃ at a rural mountain site, *Metrol.Meas. Syst.*, XXII, 25-38, 2015.

19 Li, S. M.: Equilibrium of particle nitrite with gas-phase HONO – tropospheric measurements in the high arctic
20 during sunrise, *Journal of Geophysical Research-Atmospheres*, 99, 25469-25478, 1994.

21 Li, X., Brauers, T., Haeseler, R., Bohn, B., Fuchs, H., Hofzumahaus, A., Holland, F., Lou, S., Lu, K. D., Rohrer, F.,
22 Hu, M., Zeng, L. M., Zhang, Y. H., Garland, R. M., Su, H., Nowak, A., Wiedensohler, A., Takegawa, N., Shao, M.,
23 and Wahner, A.: Exploring the atmospheric chemistry of nitrous acid (HONO) at a rural site in Southern China,
24 *Atmospheric Chemistry and Physics*, 12, 1497-1513, 2012.

25 Li, G., Su, H., Li, X., Kuhn, U., Meusel, H., Hoffmann, T., Ammann, M., Pöschl, U., Shao, M., and Cheng, Y.:
26 Uptake of gaseous formaldehyde by soil surfaces: a combination of adsorption/desorption equilibrium and chemical
27 reactions, *Atmospheric Chemistry and Physics Discussions*, 20, 16, 10299-2910311, 2016.

28 Liao, W., Case, A. T., Mastromarino, J., Tan, D., and Dibb, J. E.: Observations of HONO by laser-induced
29 fluorescence at the South Pole during ANTCI 2003, *Geophysical Research Letters*, 33, L09810, 2006.

30 Liu, Y., Han, C., Ma, J., Bao, X., and He, H.: Influence of relative humidity on heterogeneous kinetics of NO₂ on
31 kaolin and hematite, *Physical Chemistry Chemical Physics*, 17, 19424-19431, 2015.

32 Mamtimin, B., Meixner, F. X., Behrendt, T., Badawy, M., and Wagner, T.: The contribution of soil biogenic NO and
33 HONO emissions from a managed hyperarid ecosystem to the regional NO_x emissions during growing season,
34 *Atmospheric Chemistry and Physics*, 16, 10175-10194, 2016.

1 Mao, J., Ren, X., Chen, S., Brune, W. H., Chen, Z., Martinez, M., Harder, H., Lefer, B., Rappenglück, B., Flynn, J.,
2 and Leuchner, M.: Atmospheric oxidation capacity in the summer of Houston 2006: Comparison with summer
3 measurements in other metropolitan studies, *Atmospheric Environment*, 44, 4107-4115, 2010.

4 Martinez, M., Harder, H., Kubistin, D., Rudolf, M., Bozem, H., Eerdeken, G., Fischer, H., Kluepfel, T., Gurk, C.,
5 Koenigstedt, R., Parchatka, U., Schiller, C. L., Stickler, A., Williams, J., and Lelieveld, J.: Hydroxyl radicals in the
6 tropical troposphere over the Suriname rainforest: airborne measurements, *Atmospheric Chemistry and Physics*, 10,
7 3759-3773, 2010.

8 Michoud, V., Colomb, A., Borbon, A., Miet, K., Beekmann, M., Camredon, M., Aumont, B., Perrier, S., Zapf, P.,
9 Siour, G., Ait-Helal, W., Afif, C., Kukui, A., Furger, M., Dupont, J. C., Haefelin, M., and Doussin, J. F.: Study of
10 the unknown HONO daytime source at a European suburban site during the MEGAPOLI summer and winter field
11 campaigns, *Atmospheric Chemistry and Physics*, 14, 2805-2822, 2014.

12 Monge, M. E., D'Anna, B., Mazri, L., Giroir-Fendler, A., Ammann, M., Donaldson, D. J., and George, C.: Light
13 changes the atmospheric reactivity of soot, *Proceedings of the National Academy of Sciences of the United States of*
14 *America*, 107, 6605-6609, 2010.

15 Murphy, D. M., and Koop, T.: Review of the vapour pressures of ice and supercooled water for atmospheric
16 applications, *Quarterly Journal of the Royal Meteorological Society*, 131, 1539-1565, 10.1256/qj.04.94, 2005.

17 [Nägele, W., and Conrad, R.: Influence of soil pH on the nitrate-reducing microbial populations and their potential to
18 reduce nitrate to NO and N₂O, *FEMS Microbiology Letters*, 74, 49-57, 1990.](#)

19 Ndour, M., D'Anna, B., George, C., Ka, O., Balkanski, Y., Kleffmann, J., Stemmler, K., and Ammann, M.:
20 Photoenhanced uptake of NO₂ on mineral dust: Laboratory experiments and model simulations, *Geophysical*
21 *Research Letters*, 35, 2008.

22 [Novelli, A., Hens, K., Ernest, C. T., Kubistin, D., Regelin, E., Elste, T., Plass-Dulmer, C., Martinez, M., Lelieveld,
23 J., and Harder, H.: Characterisation of an inlet pre-injector laser-induced fluorescence instrument for the
24 measurement of atmospheric hydroxyl radicals, *Atmospheric Measurement Techniques*, 7, 3413-3430.](#)

25 Oswald, R., Behrendt, T., Ermel, M., Wu, D., Su, H., Cheng, Y., Breuninger, C., Moravek, A., Mougín, E., Delon,
26 C., Loubet, B., Pommerening-Roeser, A., Soergel, M., Poeschl, U., Hoffmann, T., Andreae, M. O., Meixner, F. X.,
27 and Trebs, I.: HONO Emissions from Soil Bacteria as a Major Source of Atmospheric Reactive Nitrogen, *Science*,
28 341, 1233-1235, 2013.

29 Oswald, R., Ermel, M., Hens, K., Novelli, A., Ouwersloot, H. G., Paasonen, P., Petaja, T., Sipila, M., Keronen, P.,
30 Back, J., Konigstedt, R., Beygi, Z. H., Fischer, H., Bohn, B., Kubistin, D., Harder, H., Martinez, M., Williams, J.,
31 Hoffmann, T., Trebs, I., and Soergel, M.: A comparison of HONO budgets for two measurement heights at a field
32 station within the boreal forest in Finland, *Atmospheric Chemistry and Physics*, 15, 799-813, 2015.

33 Paulson, S. E., Chung, M. Y., and Hasson, A. S.: OH radical formation from the gas-phase reaction of ozone with
34 terminal alkenes and the relationship between structure and mechanism, *Journal of Physical Chemistry A*, 103, 8125-
35 8138, 1999.

1 Pikridas, M., Bougiatioti, A., Hildebrandt, L., Engelhart, G. J., Kostenidou, E., Mohr, C., Prévôt, A. S. H.,
2 Kouvarakis, G., Zampas, P., Burkhardt, J. F., Lee, B. H., Psichoudaki, M., Mihalopoulos, N., Pilinis, C., Stohl, A.,
3 Baltensperger, U., Kulmala, M., and Pandis, S. N.: The Finokalia Aerosol Measurement Experiment – 2008 (FAME-
4 08): an overview, *Atmospheric Chemistry and Physics*, 10, 6793-6806, 2010.

5 Pitts, J. N., Sanhueza, E., Atkinson, R., Carter, W. P. L., Winer, A. M., Harris, G. W., and Plum, C. N.: An
6 investigation of the dark formation of nitrous acid in environmental chambers, *International Journal of Chemical*
7 *Kinetics*, 16, 919-939, 1984.

8 Quastel, J. H.: Soil Metabolism, *Annual Review of Plant Physiology*, 16, 217-240, 1965.

9 Ramazan, K. A., Syomin, D., and Finlayson-Pitts, B. J.: The photochemical production of HONO during the
10 heterogeneous hydrolysis of NO₂, *Physical Chemistry Chemical Physics*, 6, 3836-3843, 2004.

11 Ren, X. R., Harder, H., Martinez, M., Leshner, R. L., Oligier, A., Simpas, J. B., Brune, W. H., Schwab, J. J.,
12 Demerjian, K. L., He, Y., Zhou, X. L., and Gao, H. G.: OH and HO₂ chemistry in the urban atmosphere of New
13 York City, *Atmospheric Environment*, 37, 3639-3651, 2003.

14 Ren, X., Brune, W. H., Oligier, A., Metcalf, A. R., Simpas, J. B., Shirley, T., Schwab, J. J., Bai, C., Roychowdhury,
15 U., Li, Y., Cai, C., Demerjian, K. L., He, Y., Zhou, X., Gao, H., and Hou, J.: OH, HO₂, and OH reactivity during the
16 PMTACS-NY Whiteface Mountain 2002 campaign: Observations and model comparison, *Journal of Geophysical*
17 *Research-Atmospheres*, 111, 2006.

18 Ren, X., Gao, H., Zhou, X., Crouse, J. D., Wennberg, P. O., Browne, E. C., LaFranchi, B. W., Cohen, R. C.,
19 McKay, M., Goldstein, A. H., and Mao, J.: Measurement of atmospheric nitrous acid at Blodgett Forest during
20 BEARPEX2007, *Atmospheric Chemistry and Physics*, 10, 6283-6294, 2010.

21 Ren, X., Sanders, J. E., Rajendran, A., Weber, R. J., Goldstein, A. H., Pusede, S. E., Browne, E. C., Min, K. E., and
22 Cohen, R. C.: A relaxed eddy accumulation system for measuring vertical fluxes of nitrous acid, *Atmospheric*
23 *Measurement Techniques*, 4, 2093-2103, 2011.

24 Rubio, M. A., Lissi, E., and Villena, G.: Nitrite in rain and dew in Santiago city, Chile. Its possible impact on the
25 early morning start of the photochemical smog, *Atmospheric Environment*, 36, 293-297, 2002.

26 Sander, S. P., J. Abbatt, J. R. Barker, J. B. Burkholder, R. R. Friedl, D. M. Golden, R. E. Huie, C. E. Kolb, M. J.
27 Kurylo, G. K. Moortgat, V. L. Orkin. and P. H. Wine: *Chemical Kinetics and Photochemical Data for Use in*
28 *Atmospheric Studies*, Evaluation No. 17, JPL Publication 10-6, Jet Propulsion Laboratory, Pasadena, 2011,
29 <http://jpldataeval.jpl.nasa.gov>.

30 Scharko, N. K., Berke, A. E., and Raff, J. D.: Release of Nitrous Acid and Nitrogen Dioxide from Nitrate Photolysis
31 in Acidic Aqueous Solutions, *Environmental Science & Technology*, 48, 11991-12001, 2014.

32 Soergel, M., Regelin, E., Bozem, H., Diesch, J. M., Drennick, F., Fischer, H., Harder, H., Held, A., Hosaynali-
33 Beygi, Z., Martinez, M., and Zetzsch, C.: Quantification of the unknown HONO daytime source and its relation to
34 NO₂, *Atmospheric Chemistry and Physics*, 11, 10433-10447, 2011a.

1 Soergel, M., Trebs, I., Serafimovich, A., Moravek, A., Held, A., and Zetzsch, C.: Simultaneous HONO
2 measurements in and above a forest canopy: influence of turbulent exchange on mixing ratio differences,
3 *Atmospheric Chemistry and Physics*, 11, 841-855, 2011b.

4 Spataro, F., Ianniello, A., Esposito, G., Allegrini, I., Zhu, T., and Hu, M.: Occurrence of atmospheric nitrous acid in
5 the urban area of Beijing (China), *The Science of the total environment*, 447, 210-224, 2013.

6 Stemmler, K., Ammann, M., Donders, C., Kleffmann, J., and George, C.: Photosensitized reduction of nitrogen
7 dioxide on humic acid as a source of nitrous acid, *Nature*, 440, 195-198, 2006.

8 Stemmler, K., Ndour, M., Elshorbany, Y., Kleffmann, J., D'Anna, B., George, C., Bohn, B., and Ammann, M.: Light
9 induced conversion of nitrogen dioxide into nitrous acid on submicron humic acid aerosol, *Atmospheric Chemistry
10 and Physics*, 7, 4237-4248, 2007.

11 Stutz, J., Alicke, B., and Neftel, A.: Nitrous acid formation in the urban atmosphere: Gradient measurements of NO₂
12 and HONO over grass in Milan, Italy, *Journal of Geophysical Research-Atmospheres*, 107, 2002.

13 Su, H., Cheng, Y. F., Shao, M., Gao, D. F., Yu, Z. Y., Zeng, L. M., Slanina, J., Zhang, Y. H., and Wiedensohler, A.:
14 Nitrous acid (HONO) and its daytime sources at a rural site during the 2004 PRIDE-PRD experiment in China,
15 *Journal of Geophysical Research-Atmospheres*, 113, 2008a.

16 Su, H., Cheng, Y. F., Cheng, P., Zhang, Y. H., Dong, S., Zeng, L. M., Wang, X., Slanina, J., Shao, M., and
17 Wiedensohler, A.: Observation of nighttime nitrous acid (HONO) formation at a non-urban site during PRIDE-
18 PRD2004 in China, *Atmospheric Environment*, 42, 6219-6232, 2008b.

19 Su, H., Cheng, Y., Oswald, R., Behrendt, T., Trebs, I., Meixner, F. X., Andreae, M. O., Cheng, P., Zhang, Y., and
20 Poeschl, U.: Soil Nitrite as a Source of Atmospheric HONO and OH Radicals, *Science*, 333, 1616-1618, 2011.

21 Tang, Y., An, J., Wang, F., Li, Y., Qu, Y., Chen, Y., and Lin, J.: Impacts of an unknown daytime HONO source on
22 the mixing ratio and budget of HONO, and hydroxyl, hydroperoxyl, and organic peroxy radicals, in the coastal
23 regions of China, *Atmospheric Chemistry and Physics*, 15, 9381-9398, 2015.

24 VandenBoer, T. C., Brown, S. S., Murphy, J. G., Keene, W. C., Young, C. J., Pszenny, A. A. P., Kim, S., Warneke,
25 C., de Gouw, J. A., Maben, J. R., Wagner, N. L., Riedel, T. P., Thornton, J. A., Wolfe, D. E., Dubé, W. P., Öztürk,
26 F., Brock, C. A., Grossberg, N., Lefer, B., Lerner, B., Middlebrook, A. M., and Roberts, J. M.: Understanding the
27 role of the ground surface in HONO vertical structure: High resolution vertical profiles during NACHTT-11, *Journal
28 of Geophysical Research: Atmospheres*, 118, 10,155-110,171, 2013.

29 VandenBoer, T. C., Markovic, M. Z., Sanders, J. E., Ren, X., Pusede, S. E., Browne, E. C., Cohen, R. C., Zhang, L.,
30 Thomas, J., Brune, W. H., and Murphy, J. G.: Evidence for a nitrous acid (HONO) reservoir at the ground surface in
31 Bakersfield, CA, during CalNex 2010, *Journal of Geophysical Research-Atmospheres*, 119, 9093-9106, 2014.

32 VandenBoer, T. C., Young, C. J., Talukdar, R. K., Markovic, M. Z., Brown, S. S., Roberts, J. M., and Murphy, J. G.:
33 Nocturnal loss and daytime source of nitrous acid through reactive uptake and displacement, *Nature Geosci*, 8, 55-
34 60, 2015.

1 Villena, G., Kleffmann, J., Kurtenbach, R., Wiesen, P., Lissi, E., Rubio, M. A., Croxatto, G., and Rappenglueck, B.:
2 Vertical gradients of HONO, NO_x and O₃ in Santiago de Chile, *Atmospheric Environment*, 45, 3867-3873, 2011.

3 Vogel, B., Vogel, H., Kleffmann, J., and Kurtenbach, R.: Measured and simulated vertical profiles of nitrous acid -
4 Part II. Model simulations and indications for a photolytic source, *Atmospheric Environment*, 37, 2957-2966, 2003.

5 Wang, S. H., Ackermann, R., Spicer, C. W., Fast, J. D., Schmeling, M., and Stutz, J.: Atmospheric observations of
6 enhanced NO₂-HONO conversion on mineral dust particles, *Geophysical Research Letters*, 30, 2003.

7 Wang, L., Wang, W., and Ge, M.: Heterogeneous uptake of NO₂ on soils under variable temperature and relative
8 humidity conditions, *Journal of Environmental Sciences*, 24, 1759-1766, 2012.

9 Weber, B., Wu, D., Tamm, A., Ruckteschler, N., Rodriguez-Caballero, E., Steinkamp, J., Meusel, H., Elbert, W.,
10 Behrendt, T., Soergel, M., Cheng, Y., Crutzen, P. J., Su, H., and Poeschi, U.: Biological soil crusts accelerate the
11 nitrogen cycle through large NO and HONO emissions in drylands, *Proceedings of the National Academy of*
12 *Sciences of the United States of America*, 112, 15384-15389, 2015.

13 Wentzell, J. J. B., Schiller, C. L., and Harris, G. W.: Measurements of HONO during BAQS-Met, *Atmospheric*
14 *Chemistry and Physics*, 10, 12285-12293, 2010.

15 Wong, K. W., Tsai, C., Lefer, B., Haman, C., Grossberg, N., Brune, W. H., Ren, X., Luke, W., and Stutz, J.: Daytime
16 HONO vertical gradients during SHARP 2009 in Houston, TX, *Atmospheric Chemistry and Physics*, 12, 635-652,
17 2012.

18 Wong, K. W., Tsai, C., Lefer, B., Grossberg, N., and Stutz, J.: Modeling of daytime HONO vertical gradients during
19 SHARP 2009, *Atmospheric Chemistry and Physics*, 13, 3587-3601, 2013.

20 Yabushita, A., Enami, S., Sakamoto, Y., Kawasaki, M., Hoffmann, M. R., and Colussi, A. J.: Anion-Catalyzed
21 Dissolution of NO₂ on Aqueous Microdroplets, *The Journal of Physical Chemistry A*, 113, 4844-4848, 2009.

22 Yang, Q., Su, H., Li, X., Cheng, Y., Lu, K., Cheng, P., Gu, J., Guo, S., Hu, M., Zeng, L., Zhu, T., and Zhang, Y.:
23 Daytime HONO formation in the suburban area of the megacity Beijing, China, *Science China Chemistry*, 57, 1032-
24 1042, 2014.

25 Ye, C., Zhou, X., Pu, D., Stutz, J., Festa, J., Spolaor, M., Tsai, C., Cantrell, C., Mauldin, R. L., Campos, T.,
26 Weinheimer, A., Hornbrook, R. S., Apel, E. C., Guenther, A., Kaser, L., Yuan, B., Karl, T., Haggerty, J., Hall, S.,
27 Ullmann, K., Smith, J. N., Ortega, J., and Knote, C.: Rapid cycling of reactive nitrogen in the marine boundary layer,
28 *Nature*, 532, 489-491, 2016.

29 Young, C. J., Washenfelder, R. A., Roberts, J. M., Mielke, L. H., Osthoff, H. D., Tsai, C., Pikel'naya, O., Stutz, J.,
30 Veres, P. R., Cochran, A. K., VandenBoer, T. C., Flynn, J., Grossberg, N., Haman, C. L., Lefer, B., Stark, H., Graus,
31 M., de Gouw, J., Gilman, J. B., Kuster, W. C., and Brown, S. S.: Vertically Resolved Measurements of Nighttime
32 Radical Reservoirs; in Los Angeles and Their Contribution to the Urban Radical Budget, *Environmental Science &*
33 *Technology*, 46, 10965-10973, 2012.

1 Zhang, N., Zhou, X. L., Shepson, P. B., Gao, H. L., Alaghmand, M., and Stirm, B.: Aircraft measurement of HONO
2 vertical profiles over a forested region, *Geophysical Research Letters*, 36, 2009.

3 Zhou, X. L., Beine, H. J., Honrath, R. E., Fuentes, J. D., Simpson, W., Shepson, P. B., and Bottenheim, J. W.:
4 Snowpack photochemical production of HONO: a major source of OH in the Arctic boundary layer in springtime,
5 *Geophysical Research Letters*, 28, 4087-4090, 2001.

6 Zhou, X. L., Civerolo, K., Dai, H. P., Huang, G., Schwab, J., and Demerjian, K.: Summertime nitrous acid chemistry
7 in the atmospheric boundary layer at a rural site in New York State, *Journal of Geophysical Research-Atmospheres*,
8 107, 2002a.

9 Zhou, X. L., He, Y., Huang, G., Thornberry, T. D., Carroll, M. A., and Bertman, S. B.: Photochemical production of
10 nitrous acid on glass sample manifold surface, *Geophysical Research Letters*, 29, 2002b.

11 Zhou, X. L., Gao, H. L., He, Y., Huang, G., Bertman, S. B., Civerolo, K., and Schwab, J.: Nitric acid photolysis on
12 surfaces in low-NO_x environments: Significant atmospheric implications, *Geophysical Research Letters*, 30, 2003.

13 Zhou, X., Huang, G., Civerolo, K., Roychowdhury, U., and Demerjian, K. L.: Summertime observations of HONO,
14 HCHO, and O-3 at the summit of Whiteface Mountain, New York, *Journal of Geophysical Research-Atmospheres*,
15 112, 2007.

16 Zhou, X., Zhang, N., TerAvest, M., Tang, D., Hou, J., Bertman, S., Alaghmand, M., Shepson, P. B., Carroll, M. A.,
17 Griffith, S., Dusanter, S., and Stevens, P. S.: Nitric acid photolysis on forest canopy surface as a source for
18 tropospheric nitrous acid, *Nature Geoscience*, 4, 440-443, 2011.

19 Zhou, Y., Rosen, E. P., Zhang, H., Rattanavaraha, W., Wang, W., and Kamens, R. M.: SO₂ oxidation and nucleation
20 studies at near-atmospheric conditions in outdoor smog chamber, *Environmental Chemistry*, 10, 210-220, 2013.

21
22
23
24
25
26
27

28 **Table 1: Linear correlation factors (Pearson correlation, R²) of HONO and the unknown source S_{HONO} to meteorological**
29 **factors and different NO_x parameters.**

	during the whole campaign			
			Time of day average	
	HONO	S _{HONO}	HONO	S _{HONO}
T	0.006	0.1325	0.488	0.22714
RH	0.077	0.0045*	0.092	0.1053
Heat flux	0.261	0.300	0.617 ^c	0.64858 5 ^c

a highly correlated
R² > 0.8

b moderate correlated
R² > 0.65

J _{NO2}	0.263	0.39544 4	0.718^b	0.73567 2 ^b
NO	0.242	0.20615 4	0.857^a	0.66400 ^c
NO ₂	0.052	0.07894	0.620 ^c	0.43896
NO ₂ *RH	0.126	0.11135	0.638 ^c	0.505^c45 7
NO ₂ *RH*aerosol surface	0.095	0.44092	0.256	0.56479 ^c
NO ₂ *J	0.191	0.18964	0.828^a	0.8139^a
NO ₂ *RH*J	0.266	0.25821	0.850^a	0.8407^a
NO ₂ *RH*J*aerosol surface	0.221	0.20448	0.806^a	0.8148^a
S _{NO}		0.0120		- 0.015*0. 268

^c poorly correlated
R² > 0.5

* anti-correlated

	during the humid period				during the dry period			
	HONO	S _{HONO}	Time of day average		HONO	S _{HONO}	Time of day average	
			HONO	S _{HONO}			HONO	S _{HONO}
T	0.006	0.1216	0.031	0.1423	0.120	0.0163	0.453	-0.00445
RH	0.000	0.08192 *	0.010*	0.12746 *	0.374	0.19322 7	0.730^b	0.6083 ^{cb}
Heat flux	0.110	0.2743	0.184	0.55491 ^c	0.502 ^c	0.3035	0.685^b	0.59634 ^c
J _{NO2}	0.150	0.4657	0.245	0.69869 ^b	0.678^b	0.32057	0.829^a	0.65764^b
NO	0.168	0.18835	0.418	0.65076^b	0.487	0.32301	0.730^b	0.34029
NO ₂	0.066	0.0675	0.300	0.35326 7	0.037	-0.0023*	0.619 ^c	0.1744
NO ₂ *RH	0.084	0.04853	0.294	0.17124 5	0.161	0.0210	0.714^b	0.45236 ^c
NO ₂ *RH*aerosol surface	0.047	0.0729	0.111	0.25044 7	0.241	0.40685	0.557 ^c	0.62551 ^c
NO ₂ *J	0.214	0.2691	0.427	0.94084 5 ^a	0.358	0.0168	0.872^a	0.65703^b
NO ₂ *RH*J	0.231	0.24474	0.467	0.85077 5 ^b	0.434	0.0685	0.820^a	0.7703^b
NO ₂ *RH*J*aerosol surface	0.140	0.15260	0.465	0.78495^b	0.414	0.17130	0.664^b	0.67831 ^c b
S _{NO}		0.29432 3		0.77820^b		0.00359 3		-0.00943

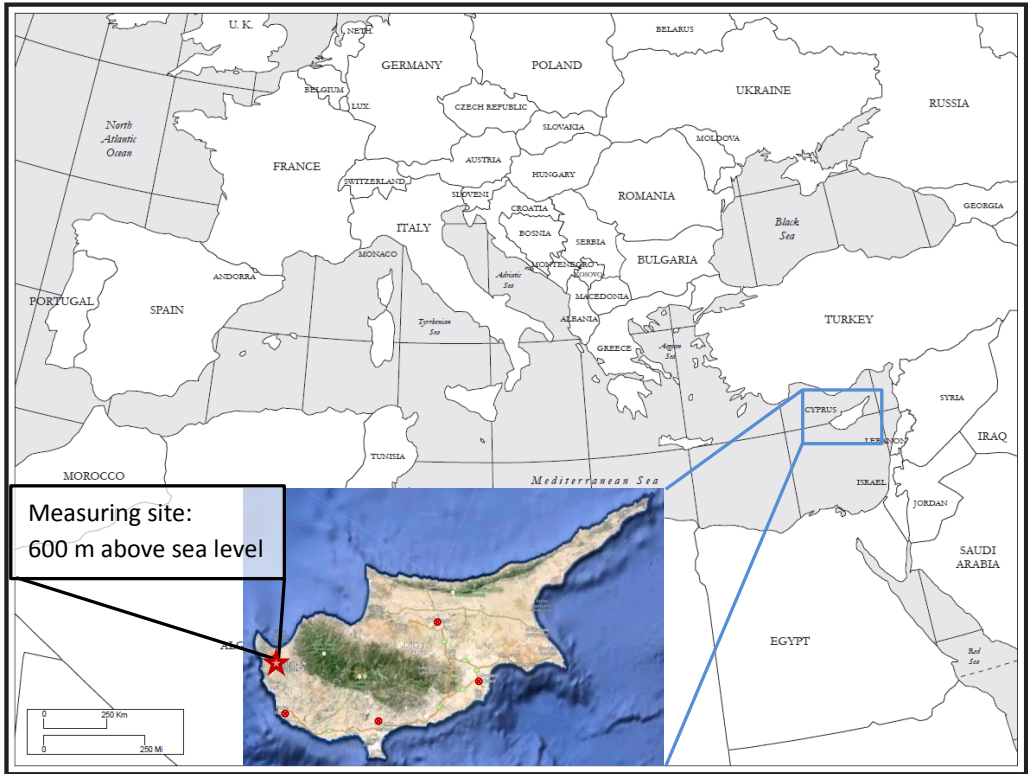


Figure 1: Map of location: the red star shows the location of Ineia and the measuring site. The four red points mark the main cities of Cyprus, Nicosia, Larnaca, Limassol and Paphos (clockwise ordering), map produced by the Cartographic Research Lab University of Alabama, map of Cyprus: google maps.

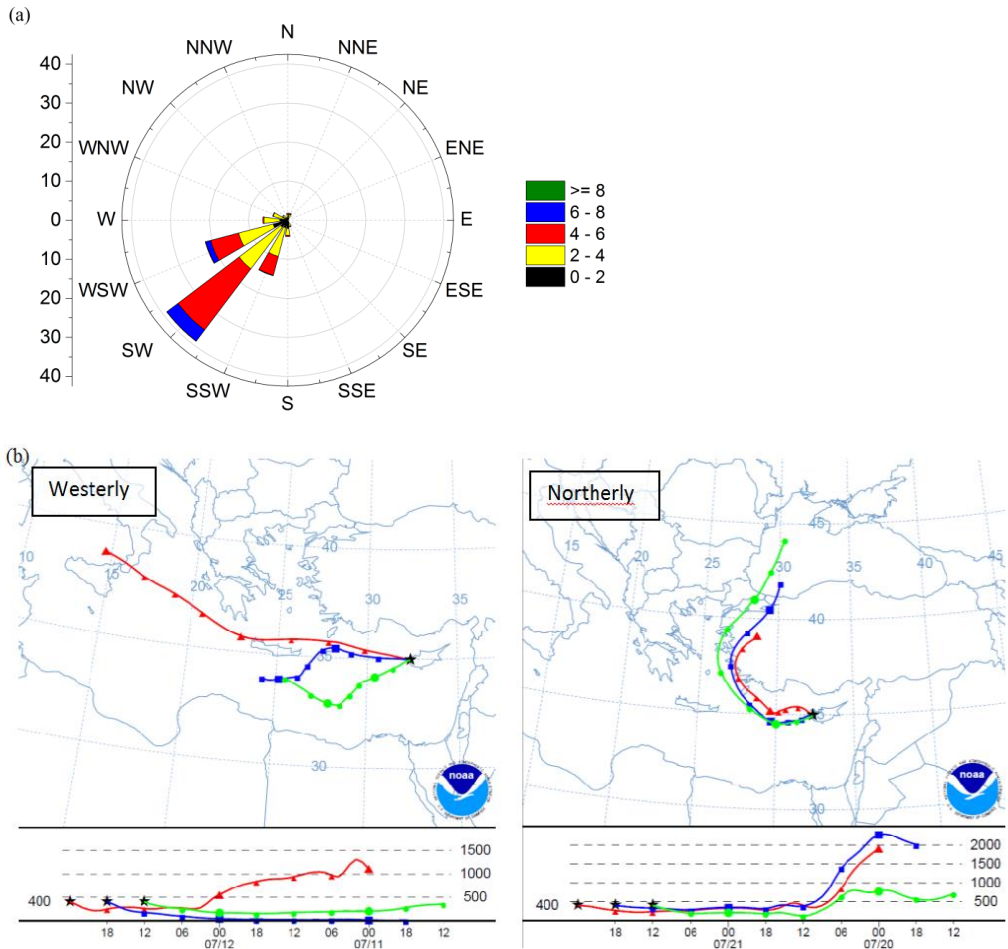


Figure 2: Airflow conditions during the CYPHEX campaign: a) Measured local wind direction, b) back trajectories calculated with NOAA Hysplit model showing examples for the two main air mass origins (48 hours, UTC = LT - 3 h).

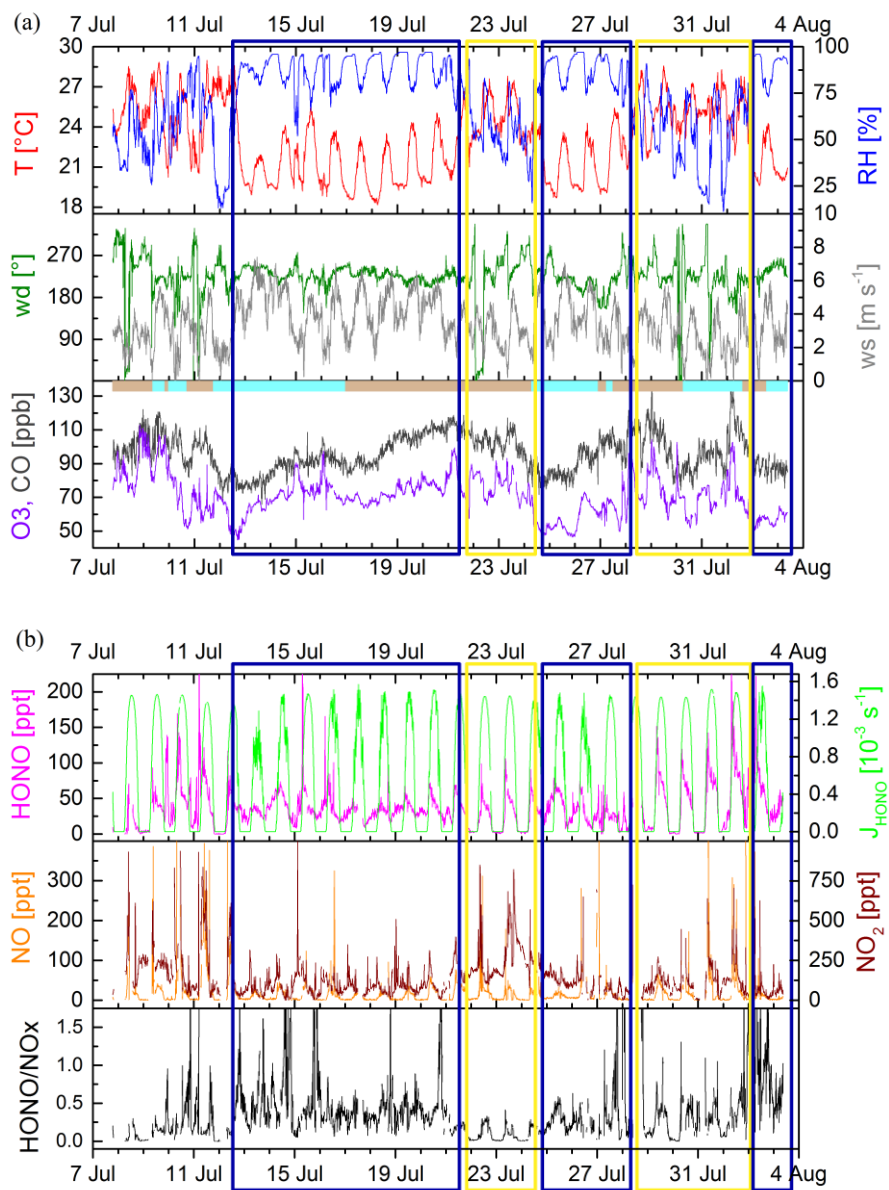
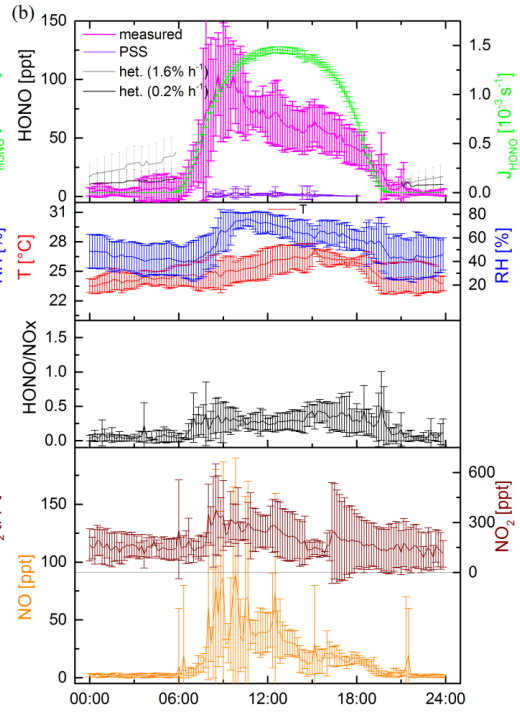
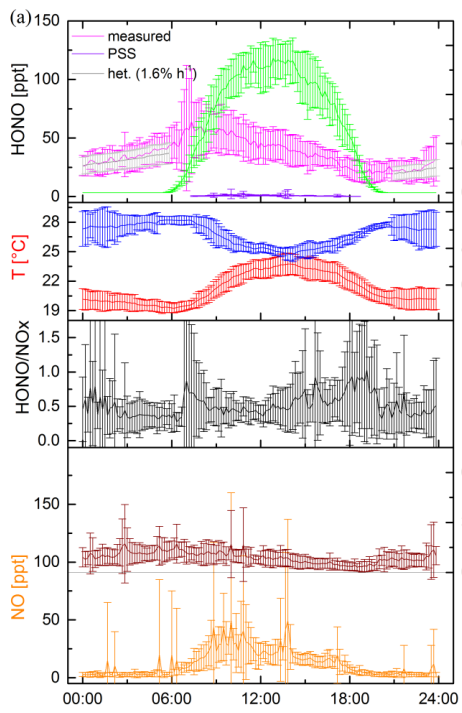


Figure 3: Measured variables during the whole campaign from 7th July to 4th August 2014, a) meteorological data (Temperature T , relative humidity RH , wind direction and speed wd , ws) and O_3 and CO indicating stable conditions, in the lower panel the bar indicates the air mass origin: bright blue = westerly, brownish = northerly, b) observed mixing ratios of $HONO$, NO_2 and NO , and the photolysis frequency J_{HONO} and the $HONO/NO_x$ ratio. The yellow and blue boxes reflect the dry and the humid periods, respectively.



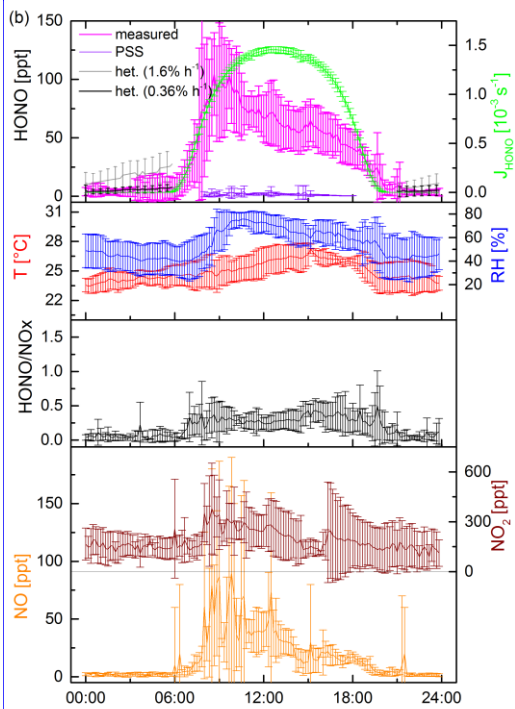


Figure 4: Diel variation of meteorological data (Temperature

T, relative humidity RH), NO and NO₂ mixing ratios, the photolysis rate for HONO J_{HONO} and HONO mixing ratios (pink: measured, violet: daytime photostationary state PSS, grey: nighttime heterogeneous NO₂ conversion) and HONO/NO_x ratio for a) average for period when RH was above 60% (blue box in Fig. 3) and b) average for dry period when RH was below 60% (yellow box in Fig. 3). Error bars represent standard deviation of diel mean.

Kommentar [HM1]: Corrected according to reviewer 1 (comment 2): changed "starting" concentration for het. Reaction calculation (both rates); (comment 8) error bars of 0.2% rate are black, and now very small -> so not possible to make it more clear

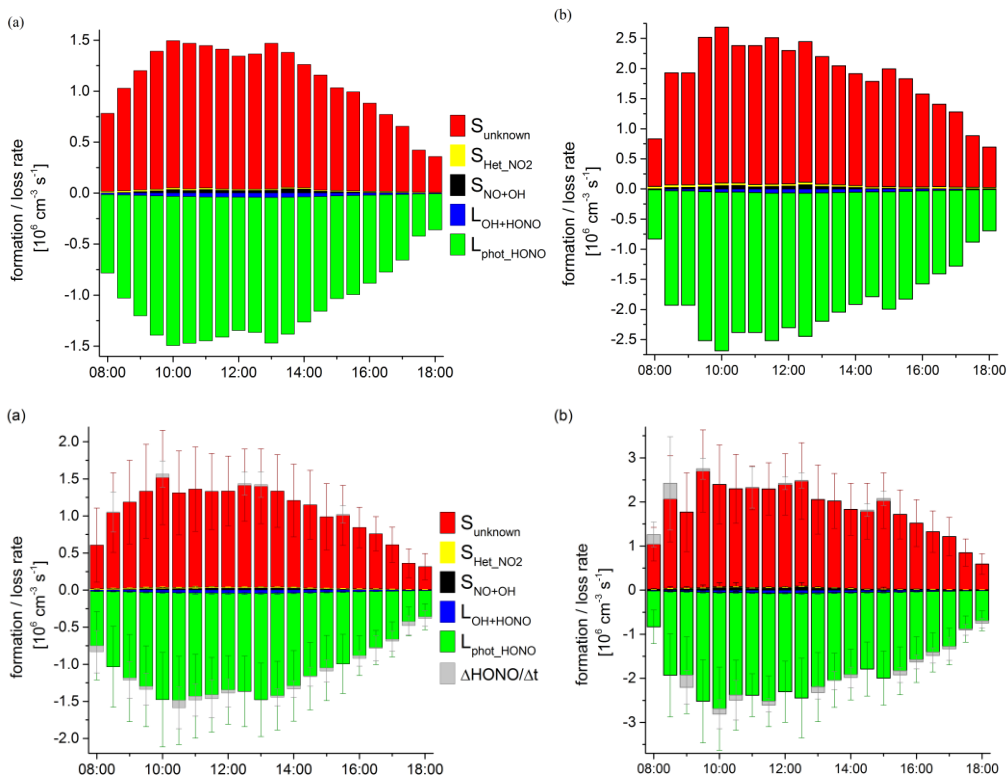


Figure 5: HONO budget analysis for a) the humid and b) the dry period. $S_{\text{OH}+\text{NO}}$ (black) stands for the formation rate of HONO via the reaction of NO and OH, $S_{\text{Het_NO}_2}$ (yellow) is the formation rate for the heterogeneous reaction of NO_2 (conversion rate $a=1.6\% \text{ h}^{-1}$; $b=0.36\% \text{ h}^{-1}$), L_{phot} (green) and $L_{\text{OH}+\text{HONO}}$ (blue) are the loss rates via photolysis and the reaction with OH and S_{unknown} is the unknown source. Error bars indicate standard deviation of diel mean.

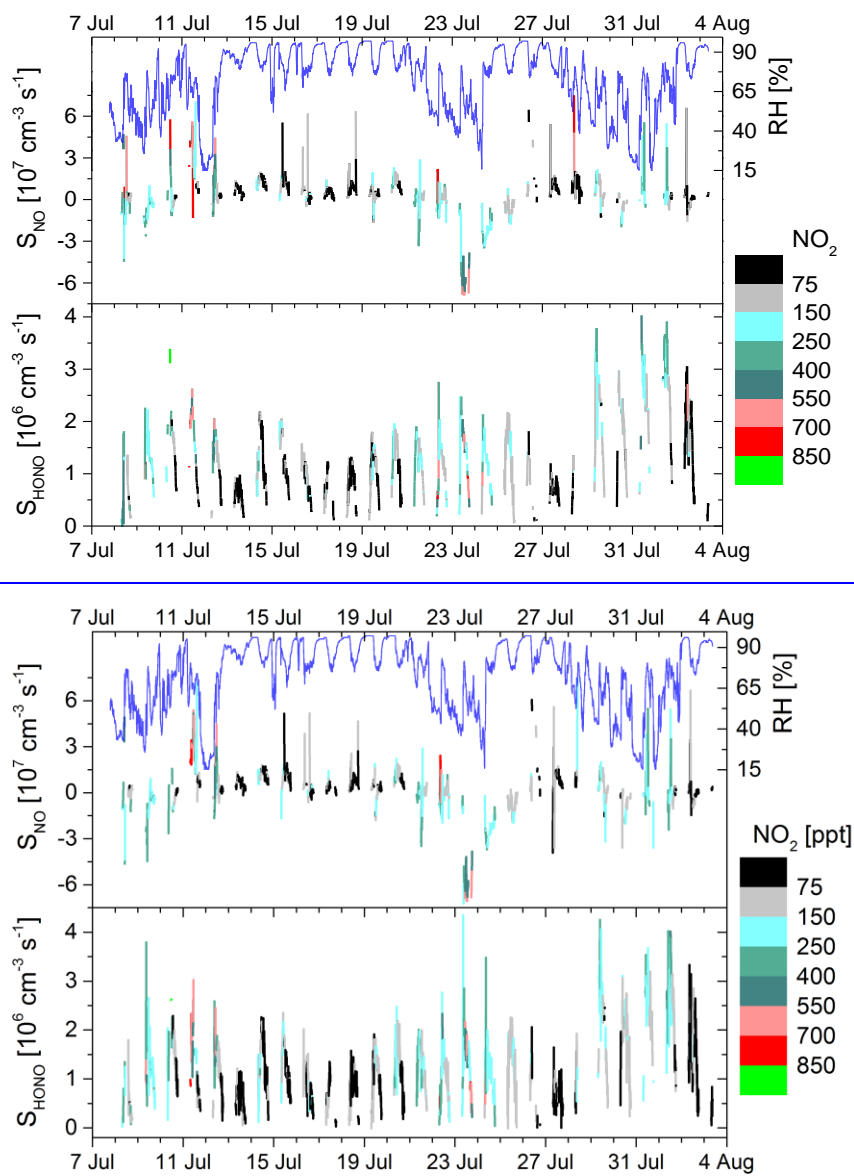


Figure 6: NO₂ (color-coded) and RH dependence of the sources of NO (S_{NO}) and HONO (S_{HONO}).

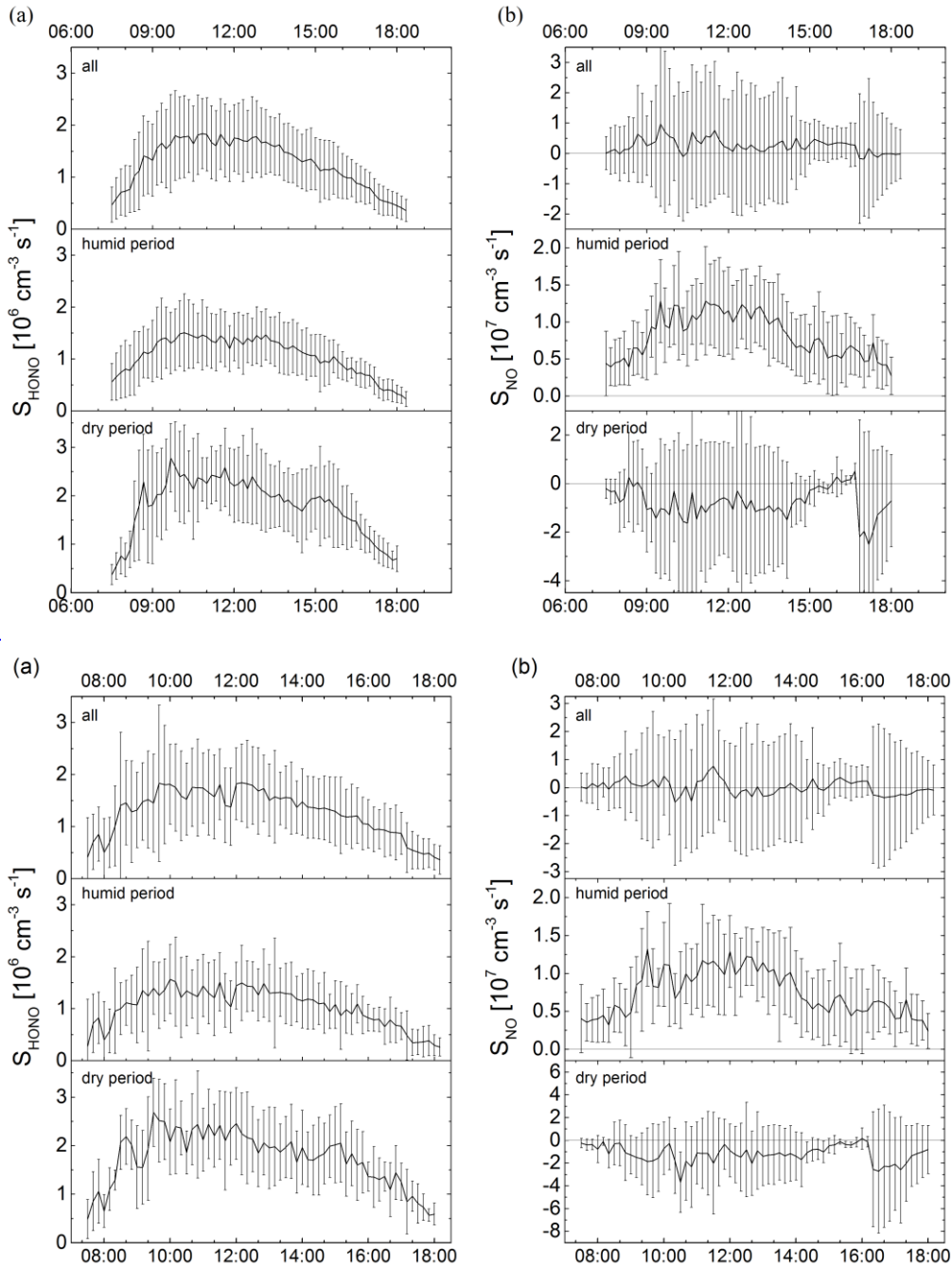
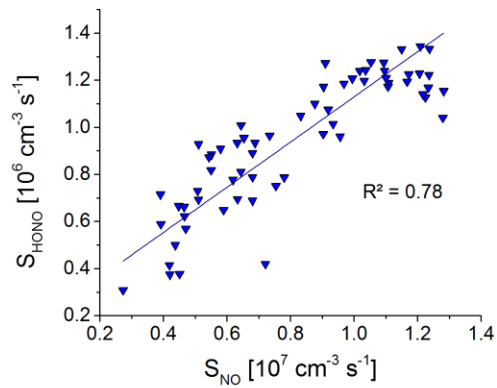
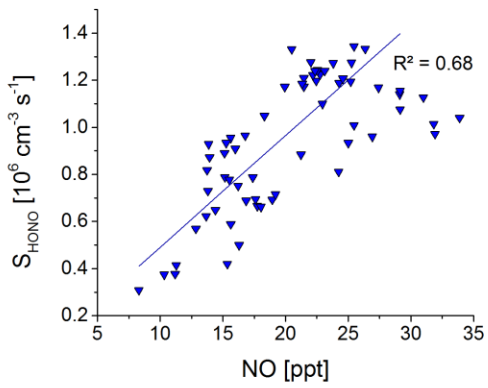
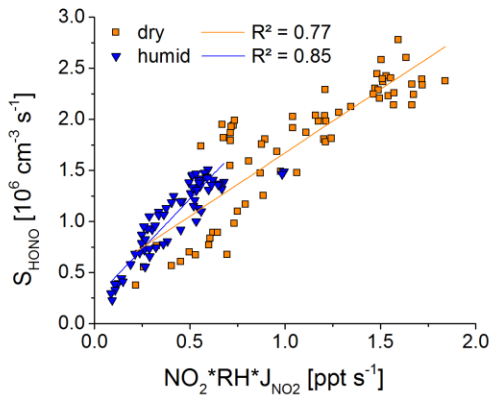
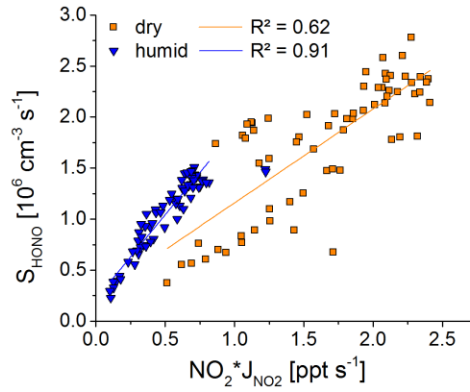
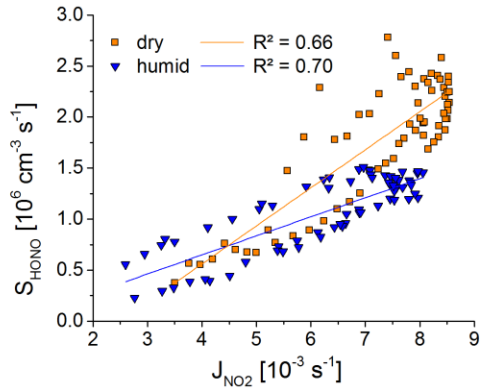


Figure 7: Diel profile of both unknown sources S_{HONO} (a) and S_{NO} (b) for all data, humid (excluding transition days: 25.7. and 2.8 and 15.7. as RH conditions changed too quickly) and dry periods. Error bars indicate standard deviation of diel average.



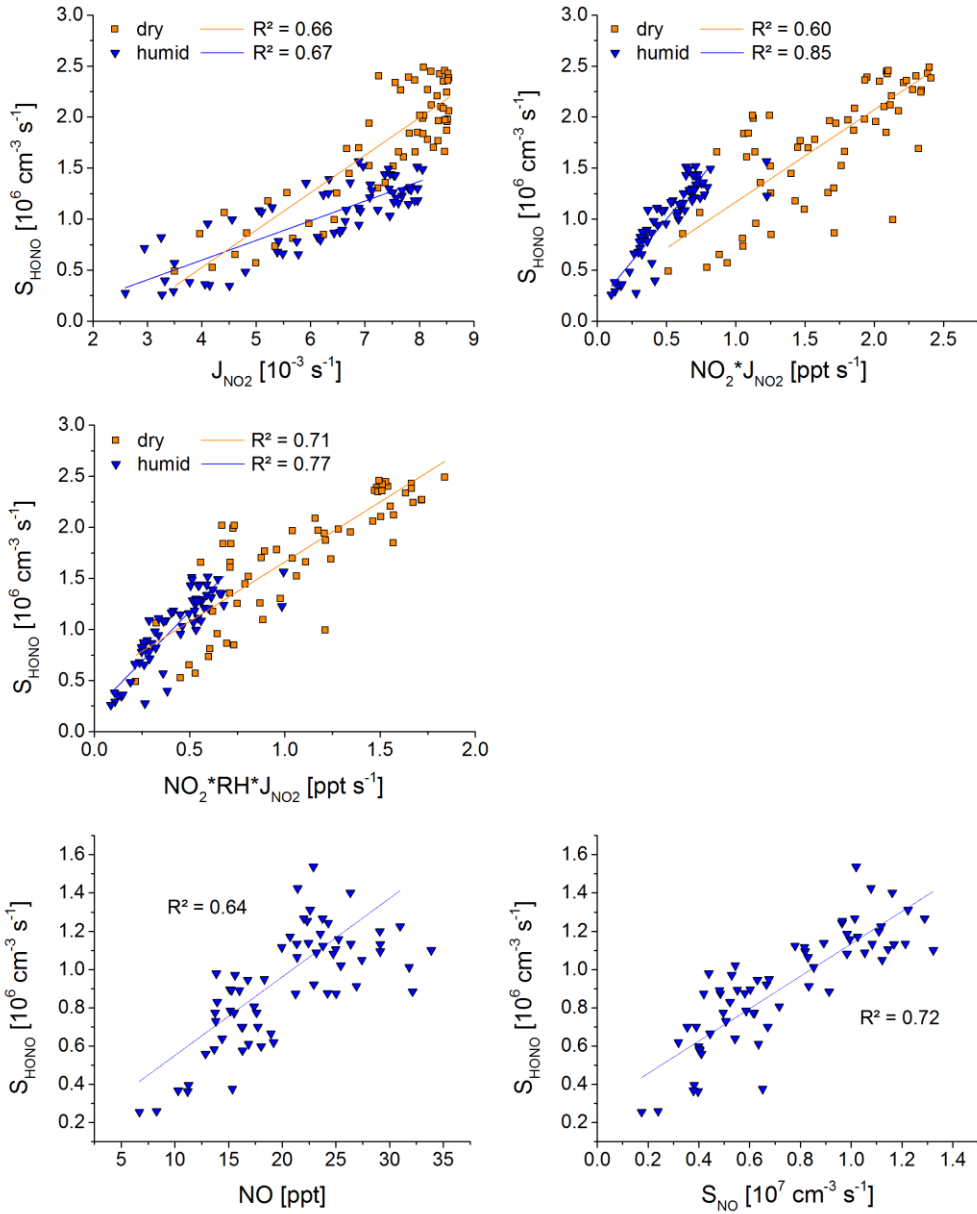


Figure 8: Correlation of S_{HONO} to light induced NO_2 reaction (for both periods, humid = blue triangle, dry = orange square), to NO and S_{NO} (only for humid period, excluding the 3 days mentioned above); time of day average data were used (S_{HONO} and NO; S_{HONO} and S_{NO} excluding the 3 days mentioned before).

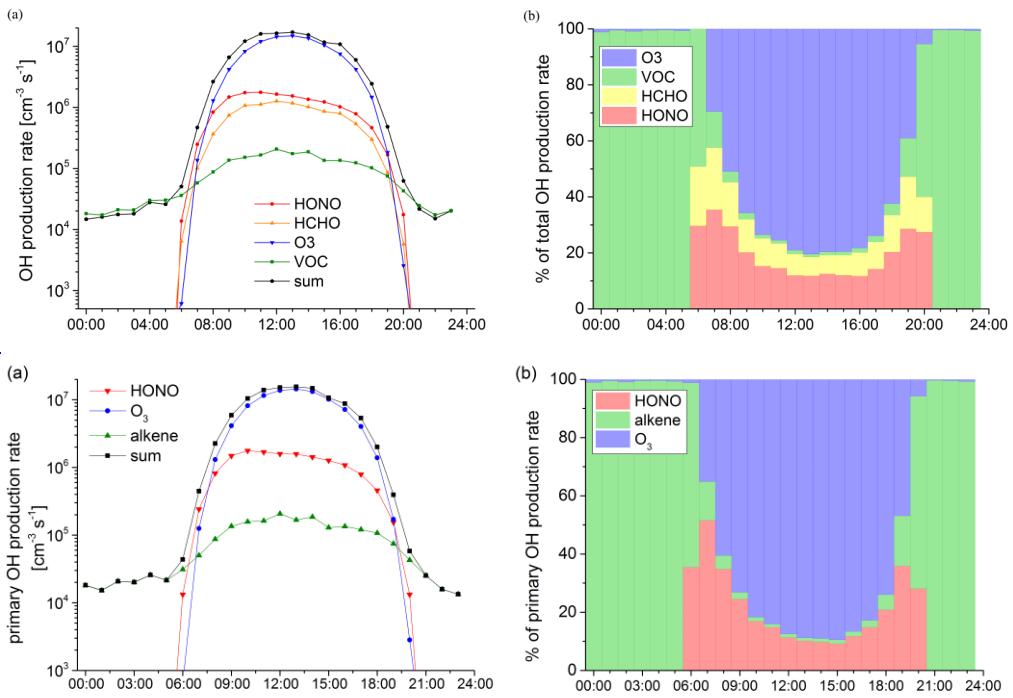


Figure 9: Average diel pattern of primary OH production from HONO, O₃, HCHO and VOCalkenes, a) shown as a) production rate and b) percentage contributions to total primary OH production.